Flanders
State of
the Art

16_023_8
FHR reports

# Ship Manoeuvring Models

Sub report 8
Free running tests with the KCS

DEPARTMENT
**MOBILITY &
PUBLIC
WORKS**

www.flandershydraulicsresearch.be

# Ship Manoeuvring Models

## Free running tests with the KCS

Delefortrie, G.; Eloot, K.; Mostaert, F.

Flanders
Hydraulics Research

Flanders
State of the Art

Cover figure © The Government of Flanders, Department of Mobility and Public Works, Flanders Hydraulics Research

## Legal notice



## Copyright and citation


D/2018/3241/153

This publication should be cited as follows:

**Delefortrie, G.; Eloot, K.; Mostaert, F.** (2018). Ship Manoeuvring Models: Free running tests with the KCS. Version 3.0. FHR Reports, 16_023_8. Flanders Hydraulics Research: Antwerp.



## Document identification

| | | | | |
|---|---|---|---|---|
| Customer: | Flanders Hydraulics Research | | Ref.: | WL2017R16_023_8 |
| Keywords (3-5): | KCS, autopilot, free running, simulation | | | |
| Text (p.): | 28 | | Appendices (p.): | 17 |
| Confidentiality: | ☒ Yes | Released as from: | | 01/01/2020 |

| | |
|---|---|
| Author(s): | Delefortrie, G. |

## Control

| | Name | Signature |
|---|---|---|
| Reviser(s): | Eloot, K. | |
| Project leader: | Delefortrie, G. | |

## Approval

| | | |
|---|---|---|
| Head of Division: | Mostaert, F. | |

# Abstract

This report discusses the execution of free running tests with the KCS in March – April 2018. Because of a new methodology and program environment, the first four chapters will deal with the execution and analysis of free running tests, including the execution of test runs. The second part of the report discusses the zigzag tests carried out with the KCS according to the SIMMAN program. Each zigzag test has been repeated at least 15 times in random order to investigate the repeatability. A comparison has been made with simulation runs, which revealed some flaws in the prediction of the rudder forces.

*Manoeuvreergedrag > Open Water > Schaalmodelproeven*

# Contents

# List of table s

# List of figures

# 1 Free running test procedure

## 1.1 Overview

Free running tests are executed with a combination of carriage control and an autopilot dynamic link library (dll). The carriage is used to position the ship in an initial position and initial velocities, after which the ship model is released and the autopilot library controls the ship model, while the carriage is used as a position tracking mechanism.

## 1.2 Autopilot library

The autopilot library, WlhAutopilot.dll, works in conjunction with the towing tank software program. However, FHR is responsible for this library. An overview of the library structure is shown in Figure 1. In this report version 2.0.6 of this C# library is considered (version 1.x being the previous C++ library).

Figure 1 – Class diagram of the WlhAutopilot.dll

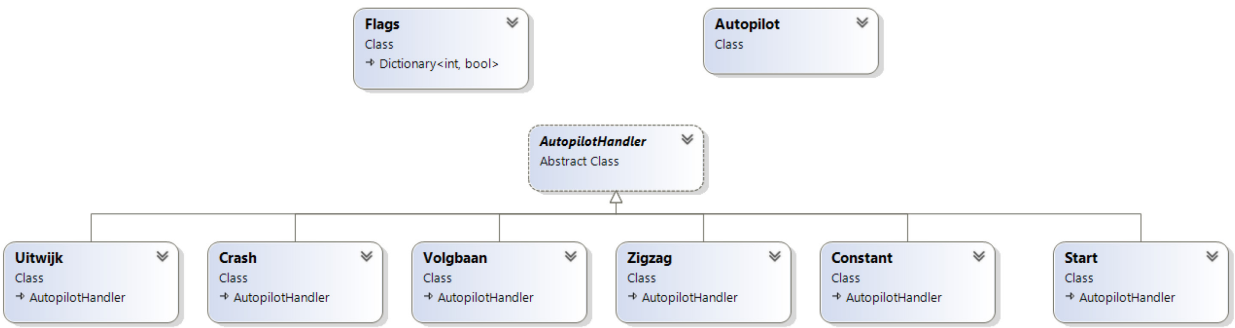


### 1.2.1 Autopilot class

#### Start of the program

The autopilot class is the communication framework or interface with the ATOS towing tank program. Every time the towing tank program is started the routine `public int GlobalInit()`is called. In this routine FHR can execute needed actions when the program is started, in particular the environmental variables are read.

#### Start of a test

If a new free running test is loaded in the ATOS towing tank program (further referred to as main program) the function `public int InitProef(string ProefBestand)` is called, with `ProefBestand` the full qualified name of the loaded test. In particular the dll will reset all variables, read the test data and decide on the type of free running test by creating a new AutopilotHandler.

### During test execution

While a test is executed the main program communicates every time step with the dll by calling its functions (see Figure 2):

- `public int SetValue(string identifier, float value)`
  For every identifier, e.g. propeller rate (ANUIT01), the main program communicates its value to the dll.
- `public int SetInfo(int flags)`
  The main program communicates the free running status to the dll, for instance: test started, free running, test aborted, … The communication is performed by passing flags, see 1.2.2.
- `public int Process()`
  Once the dll is informed with the latest status of the main program, adequate actions can be performed. The details of these actions are handled by the AutopilotHandler, see 1.2.3, a possible action for instance can be to clamp the ship model, as the free running phase has come to an end.
- `public int GetValue(string identifier, ref float value)`
  After adequate processing the dll communicates for every identifier, e.g. propeller rate (ANUIT01), its value to main program.
- `public int GetAutoPilotInfo(ref int flags)`
  The dll communicates the free running status to main program.

Figure 2 – Overview of the test process

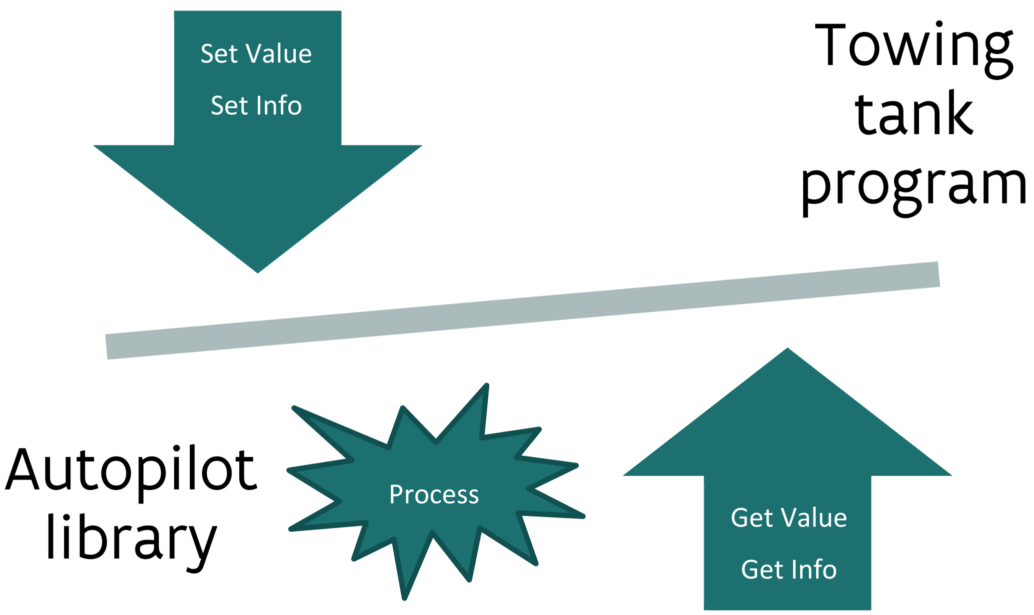


Please observe that it is crucial to use `float` instead of the standard `double` in the above described communication routines.

### 1.2.2 Flags class

The status communication between the dll and the main program is performed by a flag, which is an integer, derived from the byte representation shown in Table 1. Only the 5 last bits are of importance in the communication between the dll and the main program.

Table 1 – Flags to communicate the status between the dll and the main program

| Meaning | Motor status | | | Test started | Test aborted | Clamp | Dll aborted | Free running | int |
|---|---|---|---|---|---|---|---|---|---|
| | Not used | Not used | Not used | | | | | | |
| **Example** | 0 | 0 | 0 | 1 | 0 | 0 | 0 | 1 | = 17 |

Typical flag values during a normal test execution are:

- 16: the test has started (captive mode);
- 17: the free running mode has started;
- 21: a clamp commando has been given;
- 20: the free running mode has ended;
- 16: the ship is again in captive mode.

### 1.2.3 AutopilotHandler class

The AutopilotHandler class interpretes the auto-file and executes the necessary actions depending on the test type. The following points are common for every test type:

- In captive mode the steering signals are set to their initial values.
- In free running mode an end decision is made whether or not the ship model should be clamped. This depends on one of the following conditions:
  - a certain free running time span has passed (TVAART);
  - the ship model has reached the towing tank coordinate x = 58 m (this implies that all free running tests have to be carried out in the positive direction of the longitudinal towing tank axis);
  - the main program decides to abort the test, for instance if the ship model is going to hit the wall;
  - *other conditions, depending on the test type*.

### 1.2.4 Constant

This is the most basic autopilot handling. With this test type no actions are performed in free running mode.

### 1.2.5 Start

The aim of this test type is to accelerate the vessel starting from a given initial speed and propeller rate. An additional end condition is if the acceleration is less than 0.00025 m/s². This acceleration is always computed over the last 5 s.

Optionally the course of the vessel can be controlled during the acceleration test. To this aim a PID controller is used, which controls the rudder angle as follows:

$$-35° \leq \delta = -(K_P\psi_e \mp K_D r + K_I \int \psi_e) \leq 35° \quad (1)$$

so that the ship can follow a desired heading $\psi_e$ (PSIGEWENST). See Chapter 4 for the determination of the PID constants.

### 1.2.6 Crash

During this test the ship model has to be decelerated until zero by reversing the propeller rate. This reversal is performed in 3 steps:

- During the first 5 s of the free running phase the ship model keeps its initial propeller rate;
- The propeller is decreased at 1 rpm/ms until its magnitude is below 10 rpm. This propeller rate is maintained for a time span defined by the user (TPAUZE);
- The propeller rate is increased at 1 rpm/ms to the propeller rate of the crash stop (NCRASH).

An additional end condition is if the velocity of the longitudinal carriage is below zero. Due to the fact that all free running tests have to be carried out towards the wave maker, a crash stop starting from astern has to be carried out at a course angle of 180°.

### 1.2.7 Zigzag

The aim of the test is to execute a zigzag trajectory by reversing the rudder angle whenever a certain course angle is attained. Due to the limited width of the towing tank, the following two types are commonly executed:

- 20/5 zigzag test: rudder reversals to $\pm 20°$ are made whenever the course angle reaches $\mp 5°$;
- 10/2.5 zigzag test: rudder reversals to $\pm 10°$ are made whenever the course angle reaches $\mp 2.5°$.

The user can set an additional stopping condition by specifying the number of periods of the zigzag manoeuvre.

### 1.2.8 Uitwijk

This manoeuvre (evasive or avoidance) is quite similar to the zigzag manoeuvre, but rather to check the course angle, the yaw rate is checked, thus a 20/5 evasive test means that rudder reversals to $\pm 20°$ are made whenever the yaw rate reaches $\mp 5°/s$;

### 1.2.9 Volgbaan

#### Controller

This is the most complex free running type, in which the ship model has to travel along a number of waypoints in the towing tank. These waypoints are defined by a list of towing tank coordinates $(x_0, y_0)$, which define a linearly segmented track, which the ship will try to follow as good as possible, see Figure 3. The present controller is a modified version of the one developed in the frame of a MSc. thesis project, see (Reynvoet, 2014). The control of the rudder angle is an extended version of Eq. (1):

$$-35° \leq \delta = -\left(K_P \psi_e \mp K_D r + K_I \int_0^t \psi_e + K_Y \Delta y + K_V \left(\psi_e + \psi - \operatorname{atan}\frac{-v}{u}\right)\right) \leq 35° \quad (2)$$

See Chapter 4 for the determination of the PID constants. Additional, empirical gains are applied for drifting and cross track errors:

$$K_V \approx \frac{\delta}{\beta} = 0.05 \left(\lim_{\beta \to 0} K_V = 0\right) \quad (3)$$

$$K_Y \approx \frac{\delta}{\Delta y} = 50 \quad (4)$$

Constant values are selected for these gains, for instance a drift angle of 90° will induce an additional rudder angle of 4.5° and a cross track error of 0.7 m an additional rudder angle of 35°.

Figure 3 – Waypoint and position definition during a track control test

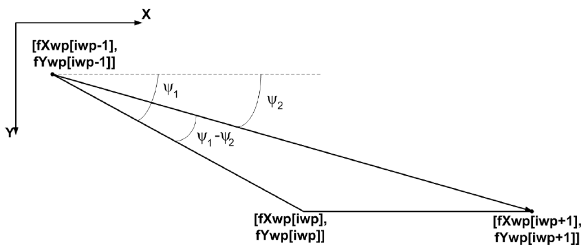


a. Definition of the segmented track, (Reynvoet, 2014)

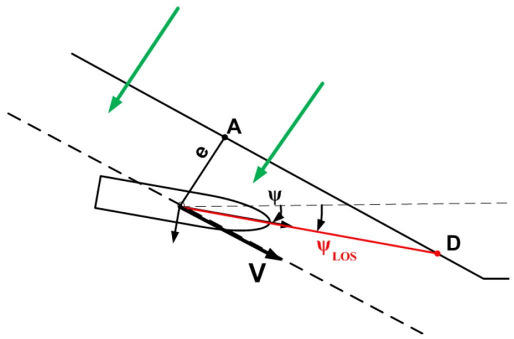


b. Position of the ship referred to the segmented track, (Reynvoet, 2014)

## Desired course angle

The desired course angle $\psi_e$ depends here on the position of the ship with respect to the segmented track. The latter is determined by the projection $A$ of the midship position to the nearest segment and the look ahead point $D$, see Figure 3b.

The orthogonal projection of the ship's position $(x, y)$ on the linear path between the previous $j-1$ and current $j$ waypoint is defined as:

$$A_x = x_0(j-1) + \frac{[(x-x_0(j-1))(x_0(j)-x_0(j-1))+(y-y_0(j-1))(y_0(j)-y_0(j-1))]}{\left[(x_0(j)-x_0(j-1))^2+(y_0(j)-y_0(j-1))^2\right]}\big(x_0(j)-x_0(j-1)\big) \quad (5)$$

$$A_y = y_0(j-1) + \frac{[(x-x_0(j-1))(x_0(j)-x_0(j-1))+(y-y_0(j-1))(y_0(j)-y_0(j-1))]}{\left[(x_0(j)-x_0(j-1))^2+(y_0(j)-y_0(j-1))^2\right]}\big(y_0(j)-y_0(j-1)\big) \quad (6)$$

The magnitude of the cross track error $\Delta y$ is consequently the distance between the ship's position and $A$. The look ahead point depends on a look ahead distance defined as:

$$L_A = \sqrt{[(\Delta y + 1.5\mathrm{L}_{PP})^2 - (\Delta y)^2]} \quad (7)$$

$$D_x = A_x + \frac{x_0(j)-x_0(j-1)}{\sqrt{\left[(x_0(j)-x_0(j-1))^2+(y_0(j)-y_0(j-1))^2\right]}} L_A \quad (8)$$

$$D_y = A_y + \frac{y_0(j)-y_0(j-1)}{\sqrt{\left[(x_0(j)-x_0(j-1))^2+(y_0(j)-y_0(j-1))^2\right]}} L_A \quad (9)$$

The desired course angle is then defined by:

$$\psi_e = \operatorname{atan}\frac{D_y - y}{D_x - x} \quad (10)$$

## Selection of the current waypoint

A point which still needs elaboration, is the selection of the current waypoint $j$. When the free running test starts, this is the second waypoint in the list. This is presently a preset position at (10,0) m, in other words, the first segment is always:

$$(x_0(0) = 0, y_0(0) = 0) \quad (11)$$

$$(x_0(1) = 10, y_0(0) = 0) \quad (12)$$

And the ship should always start its test at (0,0). When the ship is travelling along the segmented track the following options are possible:

- The previous $j-1$, current $j$ and next $j+1$ waypoint are collinear:
  - If the distance between $A$ and the current waypoint is larger than 0.5 $\mathrm{L}_{PP}$,eq. (10) can be used to determine the desired course;
  - If the distance between $A$ and the current waypoint is smaller than 0.5 $\mathrm{L}_{PP}$, the next waypoint becomes the current waypoint. A and D are evaluated versus the new current waypoint and a reevaluated eq. (10) can be used to determine the desired course;
- The waypoints are not collinear:
  - If the distance between the ship and the current waypoint is larger than $\mathrm{L}_{PP}$:
    - If $D_x$ is smaller than $x_0(j)$ : eq. (10) can be used to determine the desired course;
    - Otherwise the look ahead distance is exceeding the position of the current waypoint and a new look ahead distance should be defined, considering the next waypoint so that the ship does not deviate too much from the angular track:

$$L'_A = L_A - \sqrt{\left[(x_0(j) - A_x)^2 + \left(y_0(j) - A_y\right)^2\right]} \tag{13}$$

$$D'_x = x_0(j) + \frac{x_0(j+1) - x_0(j)}{\sqrt{\left[\left(x_0(j) - x_0(j+1)\right)^2 + \left(y_0(j) - y_0(j+1)\right)^2\right]}} L'_A \tag{14}$$

$$D'_y = y_0(j) + \frac{y_0(j+1) - y_0(j)}{\sqrt{\left[\left(x_0(j) - x_0(j+1)\right)^2 + \left(y_0(j) - y_0(j+1)\right)^2\right]}} L'_A \tag{15}$$

The desired course angle is then defined by:

$$\psi_e = \mathrm{atan}\frac{D'_y - y}{D'_x - x} \tag{16}$$

  - If the distance between the ship and the current waypoint is smaller than $\mathrm{L}_{PP}$ the next waypoint becomes the current waypoint. A and D are evaluated versus the new current waypoint and a reevaluated eq. (10) can be used to determine the desired course.

Due to the look ahead procedure sufficient waypoints have to be present, even outside the tank boundaries. The last two lines of the waypoints are typically:

$$(x_0(n-1) = 80, y_0(n-1) = 0) \tag{17}$$

$$(x_0(n) = 90, y_0(n) = 0) \tag{18}$$

### Sign of the cross track error

A last point of attention is the sign of the cross track error $\Delta y$ , which depends on the position of the ship with respect to the track. Consider the vectors defined by the track and the cross track (Figure 3b), the sign of their cross product

$$\begin{vmatrix} D_x - A_x & x - A_x \\ D_y - A_y & y - A_y \end{vmatrix} \tag{19}$$

reveals the position of the ship versus the track. A positive sign means that the ship is on the starboard side of the track, as in the example of Figure 3b. In this case $\psi_e$ should be more negative and $\Delta y$ should be considered negative in the controller equation.

## 1.3 Settings

Besides the new autopilot library the towing carriage received a new steering card (P340) and new powering since the last time free running tests have been executed. For the new steering cards new PID values have been determined for the carriage by ATOS.

For the KCS the anti-collision margin has been set at 0.35 m. This is the size of the extra envelope around the ship. Larger values are not possible in order to still be able to HOME the vessel at zero position.

In an advanced stage of the free running tests it was discovered that the roll angle as given by ATOS has a wrong sign.

# 2 User programs to process free running tests

## 2.1 ZeeMan

The output of a free running test is a DOC file (like for captive tests) and an AUTOLOG file. The latter is a 10 Hz log file from the autopilot. ZeeMan is used to transform the DOC files into KRT and HDR files. Although the name KRT suggests an averaging of measurement data, this is not performed. Like for a conventional KRT file the offsets are computed averaging the measurements during the calibration time. These offsets are then subtracted from the analogue input measurements.

The start of the KRT measurements corresponds to the time when the ship model is released, whereas the end of the measurements corresponds to the time when the clamp commando is given. Whenever the latter is not available, the end of the measurements corresponds to the last line logged.

This is the only post processing that is performed in ZeeMan 1.1.13 or above.

## 2.2 Regstatx: Free running application

### 2.2.1 Version 4.1.8

Further post processing is performed by a separate application available in Regstatx 4.1.8 or above. To enable post processing the following files need to be present in the Resources directory of Regstatx:

- KRT files in the directory KRT
- HDR files in the directory HDR
- Autolog files in the directory AutoLog
- SHP files in the directory SHP

Environment files are not needed. The free running app is started via the lighthouse icon in the upper left corner of Regstatx.

Figure 4 – Starting the free running app

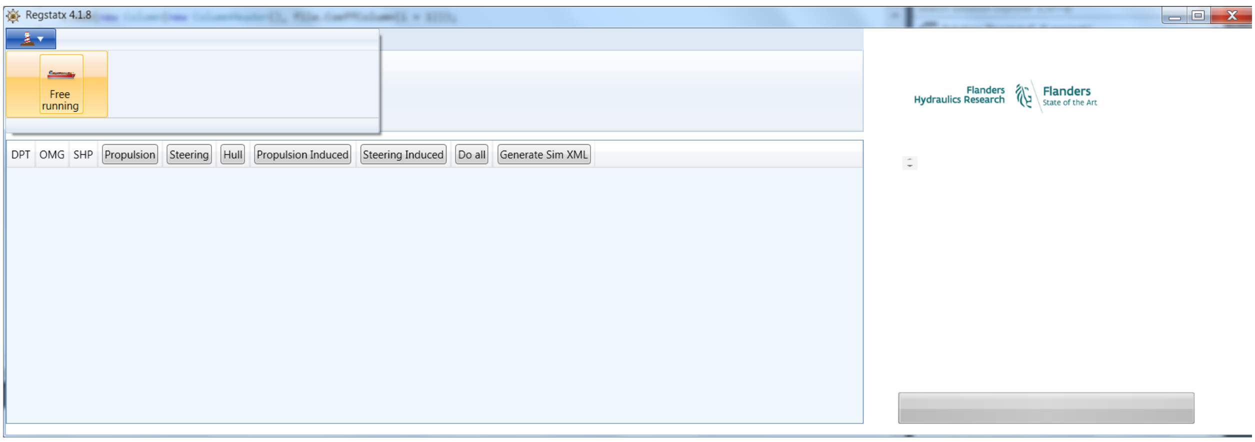


In the free running app KRT files can be loaded as shown in Figure 5. Figure 6 shows an example of the loaded KRT files. The corresponding HDR and AutoLog files are loaded as well. By clicking on the Analysis button one or all files can be analysed. The outcome of the analysis is written in the subdirectory Freerunning of Regstatx. At the same time the KRT file is updated with additional columns. More information on the computations is given in the next chapter.

Figure 5 – Loading KRT files

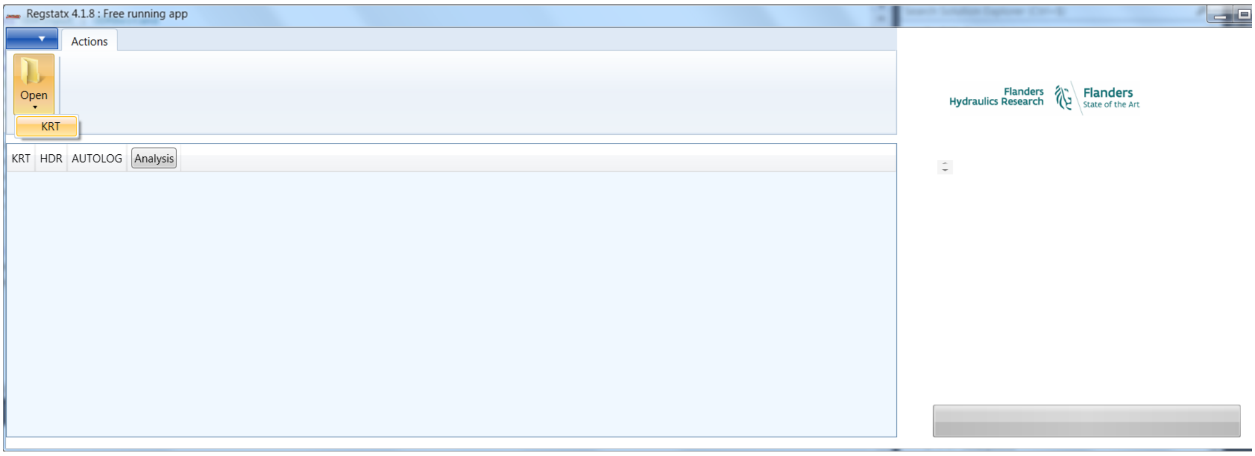


Figure 6 – Performing the analysis of free running tests

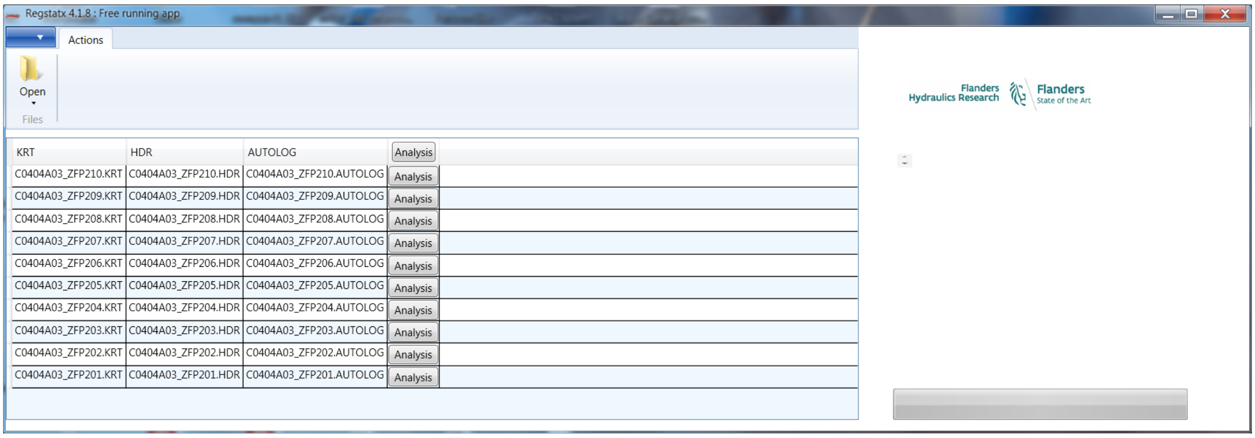


### 2.2.2 Version 4.1.9

Since version 4.1.9 free running KRT-files can be visualized as well. The loaded KRT-files can be plotted by clicking on the graph Open button of the free running app as shown in Figure 7. The free running graph window appears as shown in Figure 8.

The following user interaction is possible:

- KRT-files can be excluded from the plot by unchecking them in the upper right corner box;
- The present layout of the graph can be saved as an image to D:\Regstatx4\Graphs by clicking on the Save Graph button. The name of the graph is as follows:

  *{Name of the first KRT-file}_{Element of the X-axis}_{Element of the Y-axis}.png*

- The legends can be hidden, by checking the corresponding box. This is particularly useful if plenty of trajectories need to be plotted on a single graph;

- The lists X-axis and Y-axis determine the name of the columns that are plotted. In the example the course angle (PSI) is plotted as a function of time (TYD).

Figure 7 – Graph button

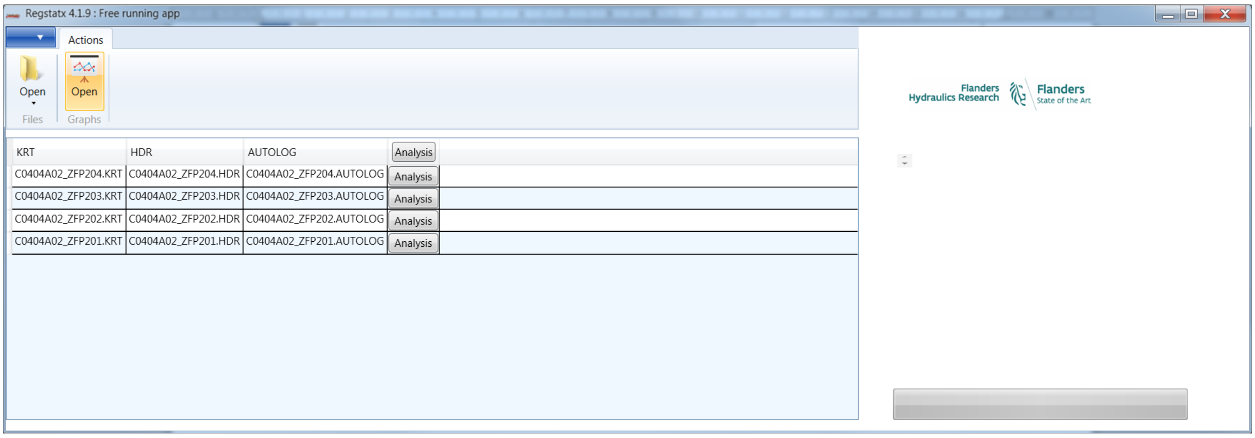


Figure 8 – Free running graph window

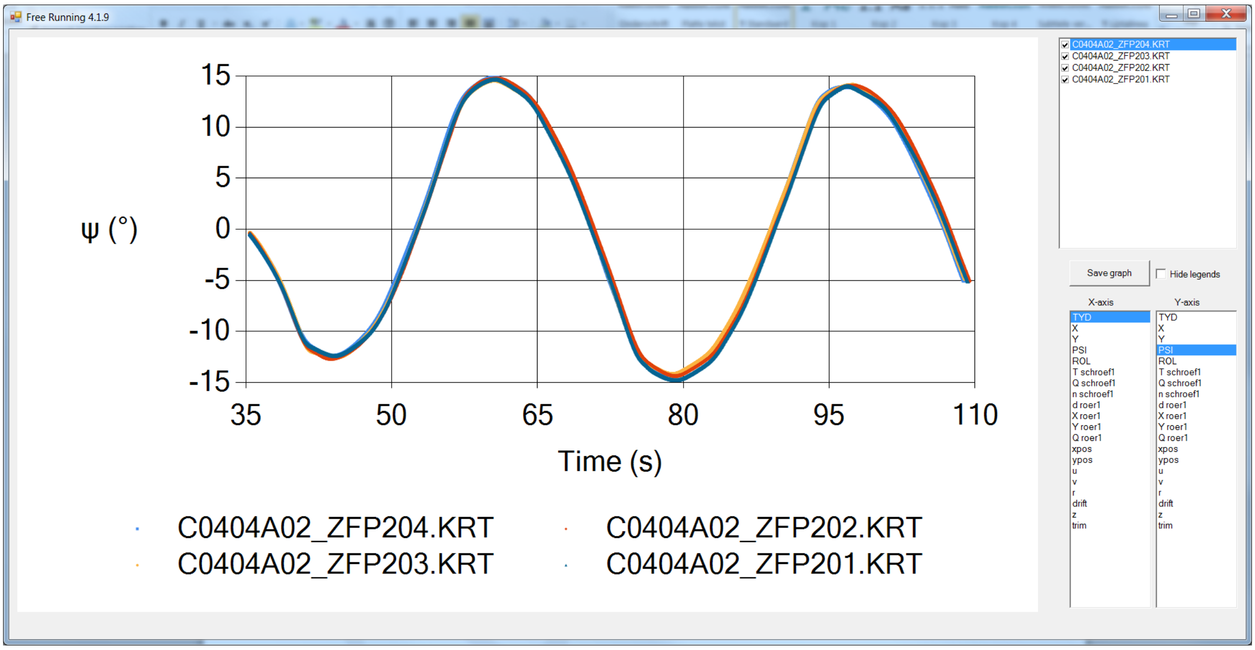

# 3 Post processing of free running tests

## 3.1 Kinematics in the horizontal plane

The horizontal position of the ship model during free running tests is given by $x_0(t)$, $y_0(t)$ and $\psi_0(t)$ in the KRT file[(1)]. The derivatives of these positions are:

$$\dot{x}_0(t_i) = \frac{x_0(t_i)-x_0(t_{i-1})}{t_i-t_{i-1}} \tag{20}$$

$$\dot{y}_0(t_i) = \frac{y_0(t_i)-y_0(t_{i-1})}{t_i-t_{i-1}} \tag{21}$$

$$\dot{\psi}_0(t_i) = \frac{\psi_0(t_i)-\psi_0(t_{i-1})}{t_i-t_{i-1}} \tag{22}$$

However, due to the too low accuracy of the $\psi_0$ measurement the value VPSI of the AutoLog file is used instead as a value for $\dot{\psi}_0(t_i) = VPSI$. Due to the mostly different logging frequency, this is an interpolated value. The global speed vector is defined as:

$$V(t_i) = \sqrt{\dot{x}_0(t_i)^2 + \dot{y}_0(t_i)^2} \tag{23}$$

while the instantaneous course of the vessel is (the derivative of the ship's track):

$$\psi_0^*(t_i) = \text{atan}\frac{\dot{y}_0(t_i)}{\dot{x}_0(t_i)} \tag{24}$$

The difference between the instant course and the course angle of the ship is the drift angle:

$$\beta(t_i) = \psi_0(t_i) - \psi_0^*(t_i) \tag{25}$$

The ship bound velocities are then:

$$u(t_i) = V(t_i)\cos\beta(t_i) \tag{26}$$

$$v(t_i) = -V(t_i)\sin\beta(t_i) \tag{27}$$

$$r(t_i) = \dot{\psi}_0(t_i) \tag{28}$$

And the ship's positional coordinates are:

$$x(t_i) = \int_0^t\left[u(t_i)\cos\left(\psi_0(t_i)\right) - v(t_i)\sin\left(\psi_0(t_i)\right)\right]dt \tag{29}$$

$$y(t_i) = \int_0^t\left[u(t_i)\sin\left(\psi_0(t_i)\right) + v(t_i)\cos\left(\psi_0(t_i)\right)\right]dt \tag{30}$$

Finally, the ship bound accelerations are:

$$\dot{u}(t_i) = \frac{u(t_i)-u(t_{i-1})}{t_i-t_{i-1}} \tag{31}$$

$$\dot{v}(t_i) = \frac{v(t_i)-v(t_{i-1})}{t_i-t_{i-1}} \tag{32}$$

$$\dot{r}(t_i) = \frac{r(t_i)-r(t_{i-1})}{t_i-t_{i-1}} \tag{33}$$

The computed values since Eq. (25) are all added as new columns to the KRT file.

---

[1] Strictly speaking these are the values of the carriage position. However the ship model is that well followed that they may be considered the position of the ship model.

## 3.2 Kinematics in the vertical plane

In theory the roll velocity and roll acceleration can be computed as well, however, due to lacking accuracy this is not performed. The position of the roll angle is given by the ATOS software. It is important to point out that the ship model has to be well balanced at the start of the free running program and that the correct offset and sign have been determined.

The sinkage of the ship model is measured by two lasers, one near the bow $f$ and another one near the stern $a$. From these two measurements the mean sinkage and trim angle can be determined:

$$z(t_i) = \frac{z_f(t_i)|x_a|+z_a(t_i)|x_f|}{|x_a|+|x_f|} \tag{34}$$

$$\vartheta(t_i) = \operatorname{atan}\frac{z_a(t_i)-z_f(t_i)}{|x_a|+|x_f|} \tag{35}$$

Both are added as new columns to the KRT file.

## 3.3 Generic output

A statistical analysis is performed on each KRT file. The results are written to a COE-file in the Freerunning subdirectory of Regstatx 4. The generic output, valid for all types of free running tests contains the following values:

- Initial values, i.e. at the start of the free running motion, of the following parameters:
  - Position of the ship in the horizontal and vertical plane;
  - Velocities in the horizontal plane;
  - Propeller rate;
  - Rudder angle.
- The final values (the last line of the KRT-file) of the same parameters.

Further parameters are added for each subtype, presented in the following paragraphs. Observe that at present no further computations are performed for the track (VOLGBAAN) type.

## 3.4 Start

The following parameters are added to the output:

- The acceleration time;
- The longitudinal acceleration distance;
- The average and standard deviation of the course angle;
- The average and standard deviation of the rudder angle.

## 3.5 Crash

The following parameters are added to the output:

- The stopping time;
- The longitudinal stopping distance;
- The lateral stopping distance or transfer;
- The rotation at stop.

## 3.6 Zigzag and Uitwijk

The following parameters are added to the output:

- The period of the zigzag test (defined as the time between the first two zero crossings of the course);
- The time until the 1st and until the 2nd course change;
- The distance until the 1st and 2nd course change;
- The time between the 1st or 2nd course change and the maximal course;
- The distance between the 1st or 2nd course change and the maximal course;
- The 1st and 2nd maximal course.

# 4 Determination of PID constants

## 4.1 Overview

The results of a zigzag test are also used to determine the PID constants. It is assumed that no manoeuvring models are available and that a 1st order Nomoto model is used to have an idea of the ship's manoeuvring behaviour:

$$r(t_i) = K\delta(t_i) - T\dot{r}(t_i) \tag{36}$$

## 4.2 Approximation of the course angle

In a first phase the measured course angle during the zigzag test is replaced by a first order harmonic approximation in order to derive a continuous yaw velocity and acceleration based on analytical expressions. The same methodology as for the analysis of oscillations in the even quadrants is used. Consequently, the initial values for the regression are determined based on a Fast Fourier Transform analysis. The input consists of $n$ time signals $t$ which are transformed to $n$ complex numbers $c = a + bi$ in the frequency domain:

- The average value is the average of the component at zero frequency: $\frac{a[0]}{n}$;
- The amplitude is the standard deviation of the time series $t$ (multiplied with $\sqrt{2}$);
- The frequency is determined by the complex number with the largest magnitude at position $i_{MAX}$:
$$\omega = \frac{2\pi}{ndt} i_{MAX} \tag{37}$$
- The phase shift is also determined by the complex number with the largest magnitude at position $i_{MAX}$:
$$\varphi_* = -\text{atan2}(b[i_{MAX}], a[i_{MAX}]) \tag{38}$$
The minus sign is needed, because the FFT is sine based, but ODRPack uses cosine.

From ODRPack an analytical expression for the course angle is obtained:

$$\psi_0(t_i) = \psi_m + \psi_a \cos(\omega t_i + \varphi) \tag{39}$$

Yielding the following velocities and accelerations:

$$r(t_i) = -\psi_a \omega \sin(\omega t_i + \varphi) \tag{40}$$

$$\dot{r}(t_i) = -\psi_a \omega^2 \cos(\omega t_i + \varphi) \tag{41}$$

## 4.3 Nomoto model

The gain $K$ and time constant $T$ of the 1st order Nomoto model are computed by the ODRPack program Nomoto.exe, using the analytical expression for the yaw velocity, yaw acceleration and the measured rudder angle.

In (Reynvoet, 2014) some empirical expressions are presented to determine PID values based on $K$ and $T$. Here the method proposed by Fossen (2018) is used. Assume a relative damping ratio $\zeta = 1$ and a bandwidth equal to:

$$\omega_b = \frac{1}{T} \tag{42}$$

The natural frequency is then:

$$\omega_n = \frac{\omega_b}{\sqrt{1-2\zeta^2+\sqrt{4\zeta^4-4\zeta^2+2}}} = \frac{\sqrt{\sqrt{2}-1}\left(\sqrt{2}+1\right)}{T} \approx \frac{1.55}{T} \tag{43}$$

Yielding the following values for the PID constants:

$$P = \left|\frac{\omega_n^2\, T}{K}\right| \approx \frac{2.40}{KT} \tag{44}$$

$$I = \frac{\omega_n}{10} P \approx \frac{0.37}{KT^2} \tag{45}$$

$$D = \left|\frac{2\zeta\omega_n T-1}{K}\right| \approx \frac{2.10}{K} \tag{46}$$

## 4.4 Application

The above methodology has been used to determine PID constants for the KCS at 50% and 20% ukc. Zigzag tests were carried out at the following propeller rates: 15%, 23%, 35%, 46% and 55% (only at 50% ukc) of the maximal propeller rate. As can be observed in Figure 9 and Figure 10 some discrepancies occur between the tests starting towards portside (positive rudder angle) and towards starboard side (negative rudder angle). These can be ascribed to the fact that a Nomoto model does not include the propeller effect. $P$ and $D$ are highly dependent of the vessel speed (in fact the rudder effect is increased due to the increased propeller rate, which means that smaller rudder angles are needed to obtain a certain course).

In order to determine an optimal model acceleration and track following tests have been carried out at different scenarios, among which:

- The values determined at a given speed were used for that given speed (only for the track following test);
- An average set of P, I and D values was used for all speeds (P = 4.0, I = 0.11 and D = 19, only for acceleration test);
- A number of scenarios have been tested with significant smaller D-values (only for acceleration test);
- A scenario in which the P and D values are determined at 1 m/s and are divided by V in the autopilot library for other speeds (with V always larger than 0.1 m/s).

In theory the first scenario should yield the best results, however, quite nervous rudder action is observed in general with the proposed D values, see for instance Figure 12b. The ship is able to follow the track with in the necessary course deviations. Lowering the D action has a direct impact on the number of rudder moves. While following a straight track as during an acceleration test, this results beneficial, because the same straightness is obtained with less rudder wear. On the other hand neglecting the D value is neither a good option, because the course deviations become too large.

In the end the last scenario was implemented in the autopilot dll. Although it works well for the acceleration tests, additional research is needed for the track follower. Ideally a new MSc. thesis could be dedicated to it.

Figure 9 – PID computations with the KCS at 50% ukc

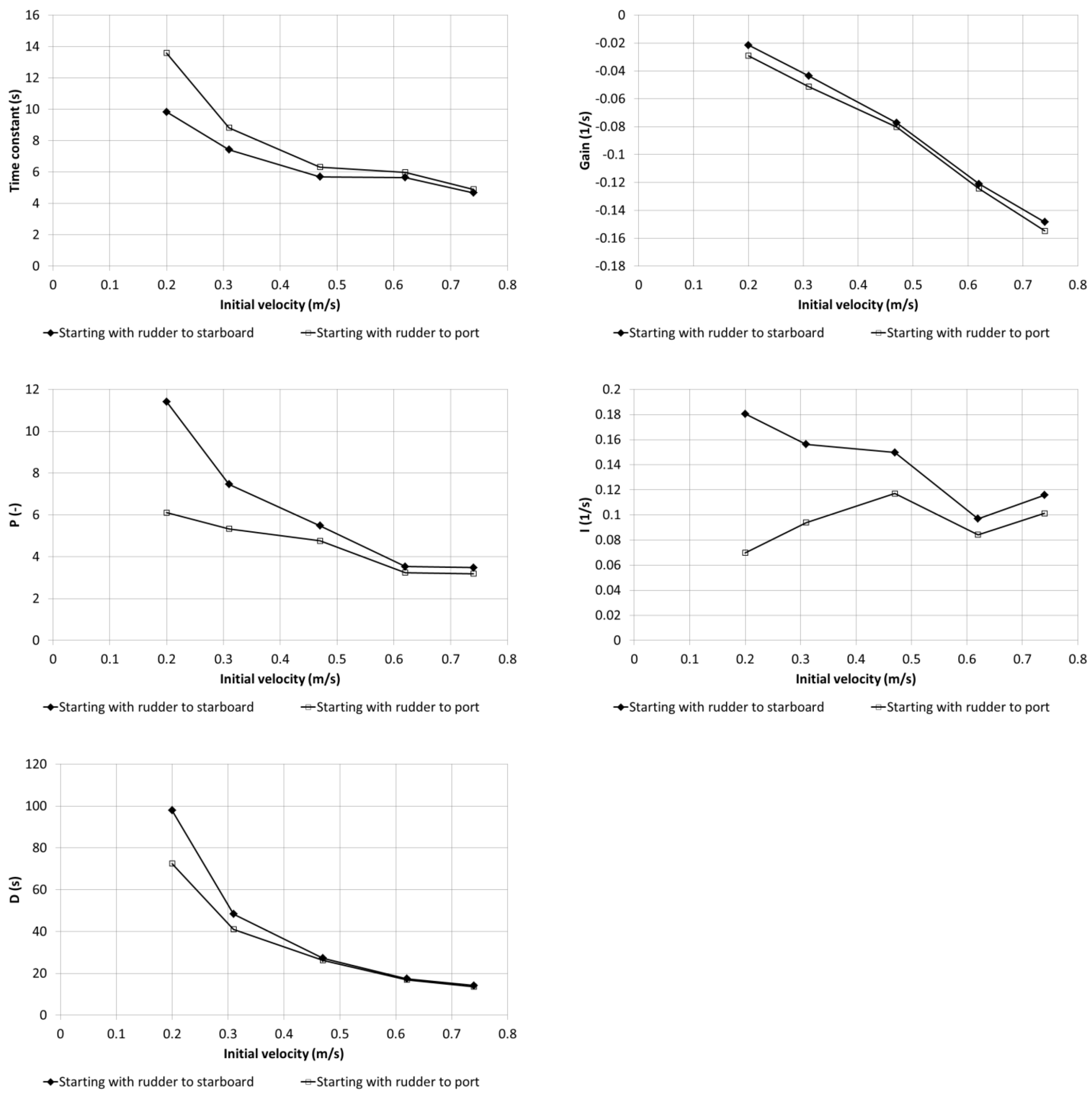

Figure 10 – PID computations with the KCS at 20% ukc

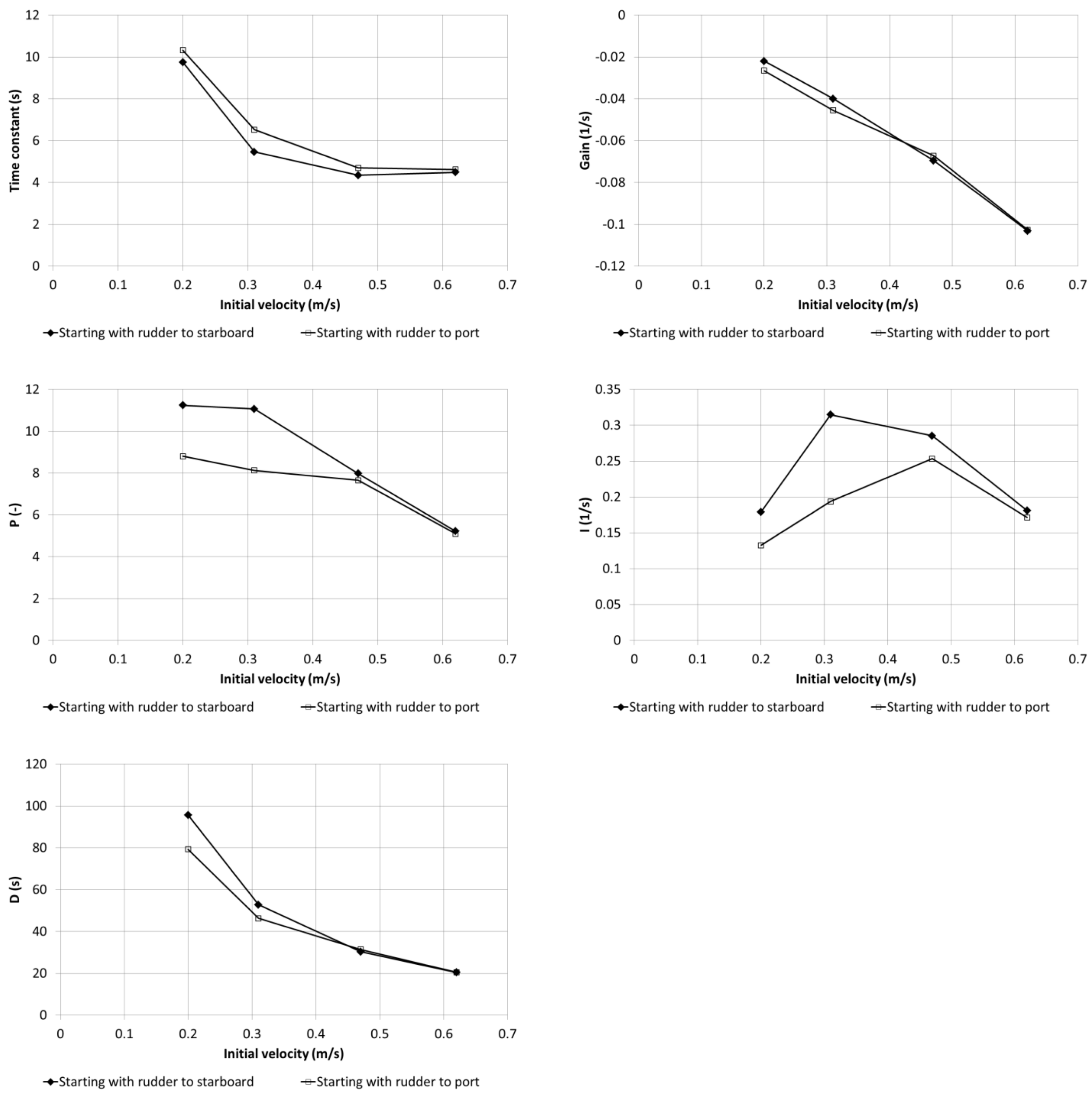

Figure 11 – Acceleration test with the KCS at 50% ukc, start speed 0.9 m/s, propeller rate 510 rpm, influence of PID values

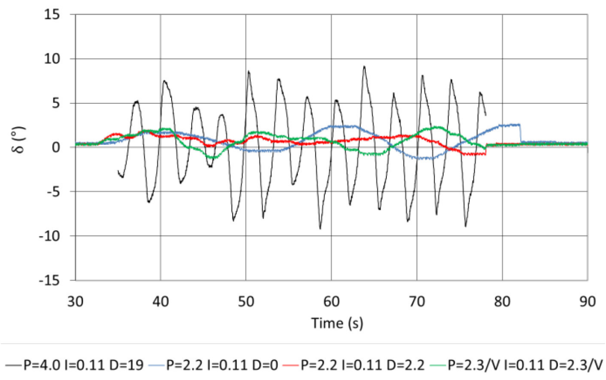


a. Rudder angle

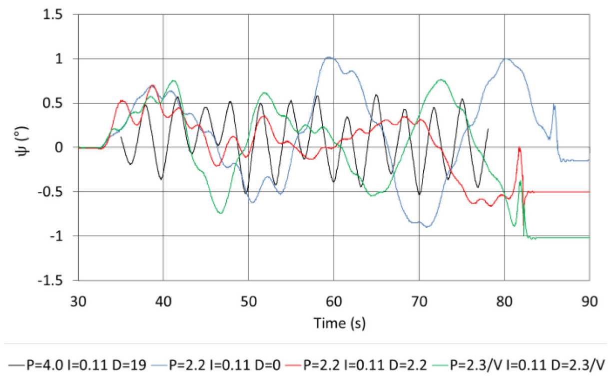


b. Course angle

Figure 12 – Track test with the KCS at 50% ukc, start speed 0.2 m/s, propeller rate 180 rpm, influence of PID values

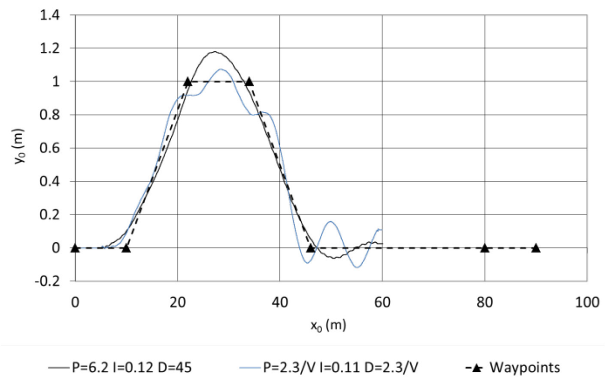


a. Track

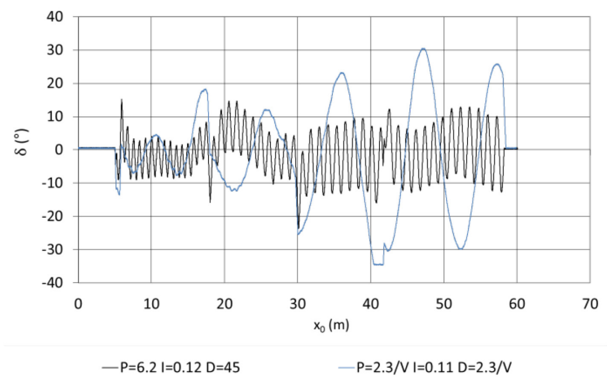


b. Rudder angle

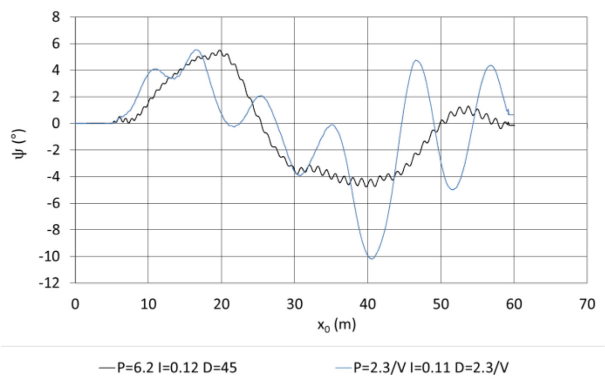


c. Course angle

# 5 Experimental program

## 5.1 Loading condition and under keel clearances

Table 2 shows the most important main particulars of the KCS (ship C04). More information can be found in [1] and [2]. The $\overline{GM}$ value is the same as applied during the tests executed in the frame of SIMMAN 2014 and has been confirmed by a heeling test.

Table 2 – Ship's main particulars (C0404)

| | Model scale | Full scale |
|---|---|---|
| $L_{PP}$ [m] | 4.367 | 230.0 |
| $B$ [m] | 0.611 | 32.2 |
| $T$ [m] | 0.2051 | 10.8 |
| $\overline{GM}$ [m] | 0.012 (±0.003) | 0.62 |
| $x_G$ [m] | -0.067 (±0.002) | -3.53 |
| $I_{XX}$ [kgm²] | 22.4 (±2) | - |
| $I_{YY}$ [kgm²] | 414.5 (±2) | - |
| $I_{ZZ}$ [kgm²] | 417.1 (±2) | - |
| $D_P$ [m] | 0.150 | 7.9 |
| $A_R$ [m²] Full | 0.0196 | 54.45 |
| Movable part | 0.0147 | 40.78 |

Free running tests have been executed at 50% ukc (C0404A02) and 20% ukc (C0404A03).

## 5.2 Executed tests

Besides the preliminary tests and the zigzag tests to determine the PID constants, the following free running tests have been executed multiple times.

### 5.2.1 Acceleration tests

Table 3 shows the acceleration tests that have been carried out, but test C0404A03_U190 has never been carried out.

Table 3 – Acceleration tests

| Name | Initial speed (m/s) | Propeller rate | Name | Initial speed (m/s) | Propeller rate |
|---|---|---|---|---|---|
| _U025 | 0.25 | 20% | _U160 | 0.60 | 50% |
| _U035 | 0.35 | 30% | _U175 | 0.75 | 60% |
| _U050 | 0.50 | 40% | _U190 | 0.90 | 70% |

### 5.2.2 Zigzag tests

Table 4 shows the zigzag tests that have been carried out, observe that these correspond to the SIMMAN conditions. Each program has been executed twice. After the first time it was discovered that the sign of the roll angle was wrong and that the ship was not sufficiently even at the start of the free running condition.

Table 4 – Zigzag tests

| 50% ukc | | | | | 20% ukc | | | | |
|---|---|---|---|---|---|---|---|---|---|
| Name | Initial speed (m/s) | Propeller rate | Type | # | Name | Initial speed (m/s) | Propeller rate | Type | # |
| _ZFM1 | 0.62 | 43.0% | -10/2.5 | 10+6 | _ZFM1 | 0.62 | 45.3% | -10/2.5 | 11+10 |
| _ZFM2 | 0.62 | 43.0% | -20/5 | 10+5 | _ZFM2 | 0.62 | 45.3% | -20/5 | 11+10 |
| _ZFP1 | 0.62 | 43.0% | 10/2.5 | 10+6 | _ZFP1 | 0.62 | 45.3% | 10/2.5 | 11+9 |
| _ZFP2 | 0.62 | 43.0% | 20/5 | 10+6 | _ZFP2 | 0.62 | 45.3% | 20/10 | 11+10 |

## 5.3 Acceleration tests

The free running time traces of some key parameters of the acceleration tests are shown in Figure 13. In order to maintain the visibility on the graphs the legends with the test names are not included, however, the same colour code has been used and the meaning can be derived from Figure 13a where a larger speed corresponds to a larger propeller rate and the lower curves for a same initial speed are always the results from 20% ukc. The course control of the vessel is in general in between +/- 0.5°, but as seen before, it gets easier at larger speeds.

The acceleration tests are mainly performed to determine the self-propulsion points for the zigzag manoeuvres. The obtained propeller-speed relationship for each under keel clearance is shown in Figure 14.

Figure 13 – Free running time traces of acceleration tests

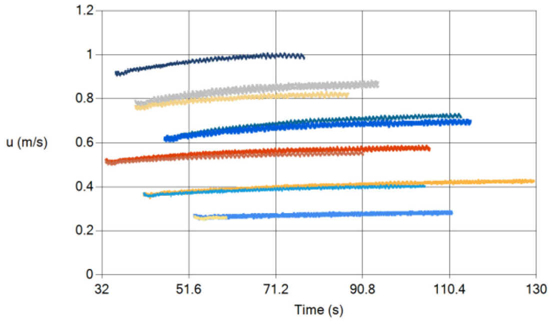


a. Longitudinal speed

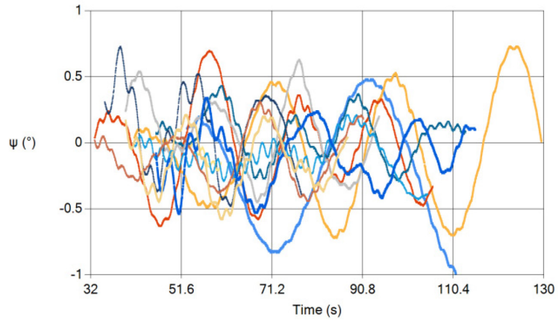


b. Course angle

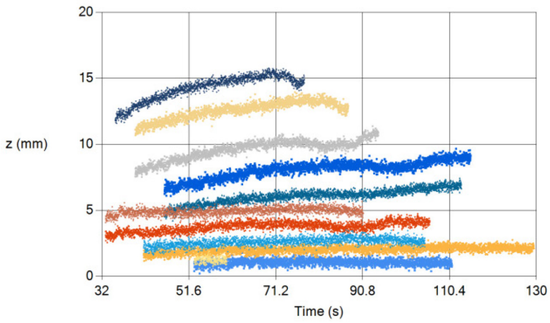


c. Mean sinkage

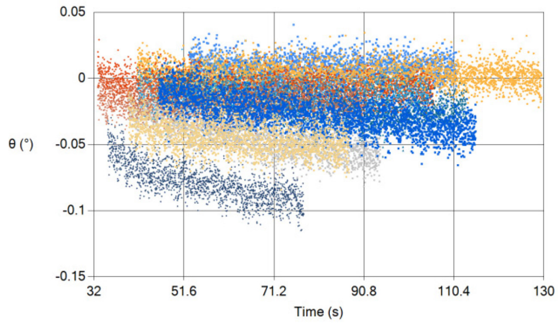


d. Pitch angle

Figure 14 – Determined self-propulsion points

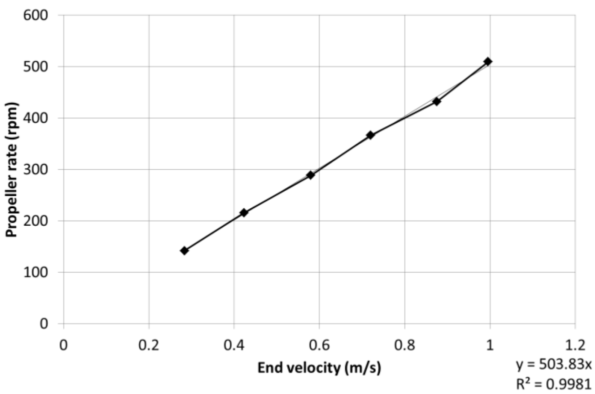


a. 50% ukc

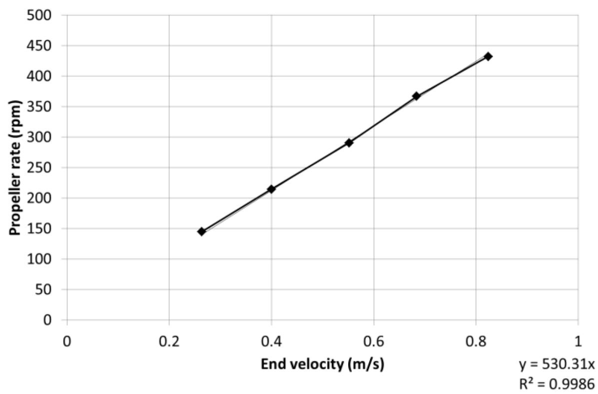


b. 20% ukc

The SIMMAN zigzag tests are carried out at an initial speed of 0.62 m/s, this means a propeller rate of:

- 312 rpm at 50% ukc (43.0%) – 0.72 rps full scale;
- 329 rpm at 20% ukc (45.3%) – 0.76 rps full scale.

The last self-propulsion point corresponds to 330 rpm that was found by BSHC at 20% ukc with the previous scale model of the KCS and with the captive model tests from 2017, but not with the captive model tests of 2010 (see Figure 15). This is as additional confirmation of the fact that the longitudinal force measured during the 2010 captive model tests was wrong. In 2010 no free running acceleration tests had been carried out.

Figure 15 - 20% ukc: measured longitudinal force in the captive model tests

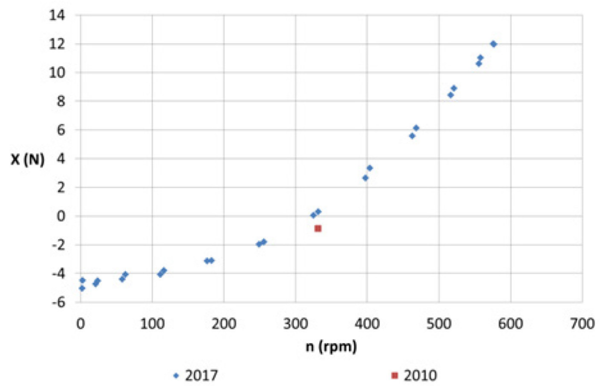


## 5.4 Zigzag tests

The time traces of some key parameters have been plotted in Appendix 1. In most cases a very good repeatability is observed. The poorest repeatability is for the ±10/2.5 zigzag tests at 20% ukc. As mentioned in section 5.2.2 the zigzag tests have been repeated, because the first set was executed with a wrong sign of the roll angle and with a roll offset. All previous graphs have shown all sets, however in Figure 16 the effect of the different roll angles is made clear for the 20/5 zigzag test at 20% ukc. A negative roll angle is expected whenever the rudder angle is positive, which is the case for the most recent tests. Mind also that a clear offset was present in the first set. This offset has a slight influence on the statistical outcome of the zigzag test. According to ATOS the way the roll angle was measured did not change since the free running system was built, in other words, probably all free running tests performed up till now have a wrong sign of the roll angle.

Figure 16 - Free running roll angles of 20/5 zigzag tests at 20% ukc

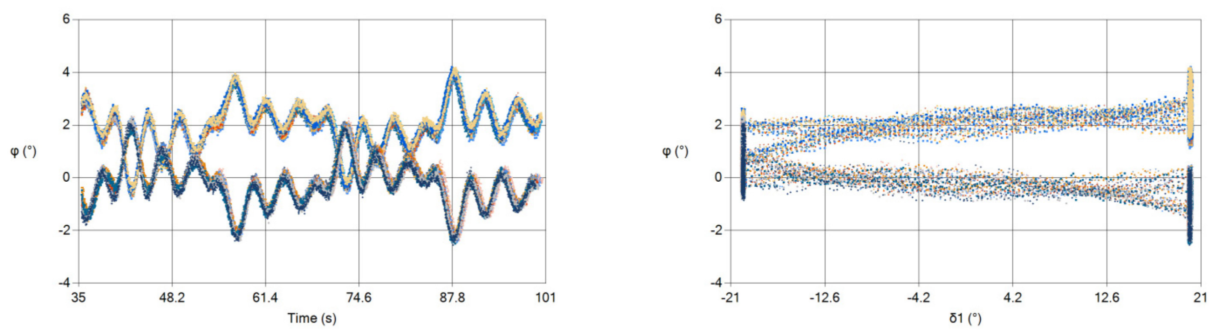


a. As a function of time

b. As a function of rudder angle

The statistics are also shown in Appendix 1, namely the period and the maximally attained course angles during all zigzag tests. For some zigzag tests and for some parameters a significant difference can be seen before and after the roll checks were made, which indicates that the initial heel angle of the ship has an influence on the outcome of the test. The averages and standard deviations of all the runs are shown in

Table 5 to Table 8. Parameters that have a significantly different magnitude when starting to port or to starboard have been underlined. This is always the case for the first overshoot angle.

Table 5 – Key parameters of 10/2.5 zigzag tests at 50% ukc

| Parameter | Starting to port | | | Starting to starboard | | |
|---|---|---|---|---|---|---|
| | All | Before roll checking | After roll checking | All | Before roll checking | After roll checking |
| Period (s) | 41.4 ± 0.3 | 41.3 ± 0.3 | 41.5 ± 0.2 | 41.8 ± 0.5 | 41.5 ± 0.2 | 42.3 ± 0.4 |
| Overshoot 1 (°) | -3.6 ± 0.1 | -3.7 ± 0.1 | -3.6 ± 0.1 | 3.1 ± 0.1 | 3.0 ± 0.1 | 3.1 ± 0.1 |
| Overshoot 2 (°) | 7.2 ± 0.2 | 7.2 ± 0.2 | 7.2 ± 0.3 | -7.3 ± 0.2 | -7.3 ± 0.1 | -7.4 ± 0.3 |

Table 6 – Key parameters of 20/5 zigzag tests at 50% ukc

| Parameter | Starting to port | | | Starting to starboard | | |
|---|---|---|---|---|---|---|
| | All | Before roll checking | After roll checking | All | Before roll checking | After roll checking |
| Period (s) | 36.5 ± 0.2 | 36.5 ± 0.2 | 36.6 ± 0.1 | 36.5 ± 0.2 | 36.5 ± 0.2 | 36.6 ± 0.2 |
| Overshoot 1 (°) | -7.5 ± 0.1 | -7.5 ± 0.1 | -7.6 ± 0.2 | 6.9 ± 0.1 | 6.9 ± 0.1 | 6.9 ± 0.2 |
| Overshoot 2 (°) | 9.8 ± 0.2 | 9.7 ± 0.1 | 9.9 ± 0.3 | -10.7 ± 0.2 | -10.7 ± 0.2 | -10.8 ± 0.2 |

Table 7 – Key parameters of 10/2.5 zigzag tests at 20% ukc

| Parameter | Starting to port | | | Starting to starboard | | |
|---|---|---|---|---|---|---|
| | All | Before roll checking | After roll checking | All | Before roll checking | After roll checking |
| Period (s) | 30.6 ± 0.5 | 30.8 ± 0.4 | 30.4 ± 0.6 | 30.8 ± 0.3 | 30.8 ± 0.3 | 30.9 ± 0.4 |
| Overshoot 1 (°) | -2.6 ± 0.1 | -2.5 ± 0.1 | -2.7 ± 0.1 | 2.0 ± 0.2 | 2.1 ± 0.1 | 1.9 ± 0.1 |
| Overshoot 2 (°) | 3.9 ± 0.2 | 4.0 ± 0.2 | 3.7 ± 0.2 | -3.7 ± 0.2 | -3.6 ± 0.2 | -3.9 ± 0.2 |

Table 8 – Key parameters of 20/5 zigzag tests at 20% ukc

| Parameter | Starting to port | | | Starting to starboard | | |
|---|---|---|---|---|---|---|
| | All | Before roll checking | After roll checking | All | Before roll checking | After roll checking |
| Period (s) | 30.9 ± 0.2 | 31.0 ± 0.2 | 30.8 ± 0.2 | 30.9 ± 0.1 | 30.8 ± 0.1 | 30.9 ± 0.1 |
| Overshoot 1 (°) | -5.0 ± 0.2 | -4.9 ± 0.1 | -5.2 ± 0.1 | 4.9 ± 0.2 | 5.0 ± 0.2 | 4.7 ± 0.1 |
| Overshoot 2 (°) | 6.3 ± 0.2 | 6.4 ± 0.1 | 6.2 ± 0.2 | -6.4 ± 0.2 | -6.2 ± 0.2 | -6.6 ± 0.1 |

# 6 Simulations

## 6.1 Overview

Identical free running tests have been carried out on the simulator and are compared to the new set of free running tests. The used methodology is the same as in (Delefortrie *et al.*, 2018), more specifically the comparisons are performed on prototype scale and care is taken of the initial conditions. As the repeatability is guaranteed the tank tests shown in Table 9 have been selected for comparison. For the selected runs in which the roll angle had the wrong sign, the sign of the roll was corrected.

Table 9 – Initial conditions of the simulation runs

| Test name | ukc | Type | $u_{initial}$ (m/s) | $v_{initial}$ (m/s) | $r_{initial}$(°/s) |
|---|---|---|---|---|---|
| C0404A02_ZFP204 | 50% | 20/5 | 4.62 | 0.01 | -0.1357 |
| C0404A02_ZFM204 | 50% | -20/5 | 4.61 | -0.11 | 0.1065 |
| C0404A02_ZFM104 | 50% | -10/2.5 | 4.64 | -0.08 | 0.0610 |
| C0404A02_ZFP104 | 50% | 10/2.5 | 4.62 | 0.03 | -0.0851 |
| C0404A03_ZFM210 | 20% | -20/5 | 4.56 | -0.02 | 0.0858 |
| C0404A03_ZFM120 | 20% | -10/2.5 | 4.59 | -0.05 | 0.0520 |
| C0404A03_ZFP118 | 20% | 10/2.5 | 4.59 | -0.10 | -0.0813 |
| C0404A03_ZFP215 | 20% | 20/5 | 4.56 | -0.00 | -0.1154 |

The values for the initial lateral velocity have not been considered due to their relatively large uncertainty. Mind that the initial course angle during the tank tests was not always zero, however, this could not be accounted for in the simulator, because the course deviations are expressed relatively to the initial course angle, whereas in the towing tank the course deviations are always absolute.

## 6.2 Results

Appendix 2 contains the graphs of the comparisons. The agreement between simulations and free running tests is excellent for the roll, heave and pitch motions. However, as can be observed for both 20% and 50% ukc, the simulations predict quicker manoeuvres compared to the free running tests. Both the period and the overshoots are considerably smaller than in the free running tests. To investigate the reasons for this, more parameters than the ones shown in Appendix 2 have been plotted. Figure 17 shows for instance the lateral rudder force during a zigzag manoeuvre. As can be seen during the simulation larger peaks are reached with every rudder reversal compared to the free running tank test. After a while both forces seem to converge again. Such behaviour can be observed for all zigzag tests. A possible hypothesis is that in a free running test, the flow has to settle before adapting to the value of the new rudder angle, while in a simulator this happens at once. The question is whether this is only limited to model scale, or whether this also happens on full scale (different time interval and duration). It is a fact that the period can be matched by adapting the average value of the lateral rudder force only, see Table 10, which has been used to plot the tuned simulation series in Appendix 2. If the same multiplicator is used for the longitudinal rudder force then the speed decrease also shows more agreement with the free running tests. On the other hand the sway drift force has been decreased to better match the sway velocity and the overshoots, however, especially for the 10/2.5 manoeuvres, the latter are hard to match.

Table 10 – Applied tuning to the simulations

| Parameter | ukc | Multiplicator | Remark |
|---|---|---|---|
| $Y'(\beta)$ | 50% and 20% | 0.6 | Increases the overshoots |
| $F_X$ | 50% | 0.8 | Lowers the velocity decrease |
| | 20% | 0.6 | |
| $F_Y$ | 50% | 0.8 | Increases the period |
| | 20% | 0.6 | |

Figure 17 – Lateral force acting on the rudder, C0404A02_ZFP104, 10/2.5 zigzag at 50% ukc

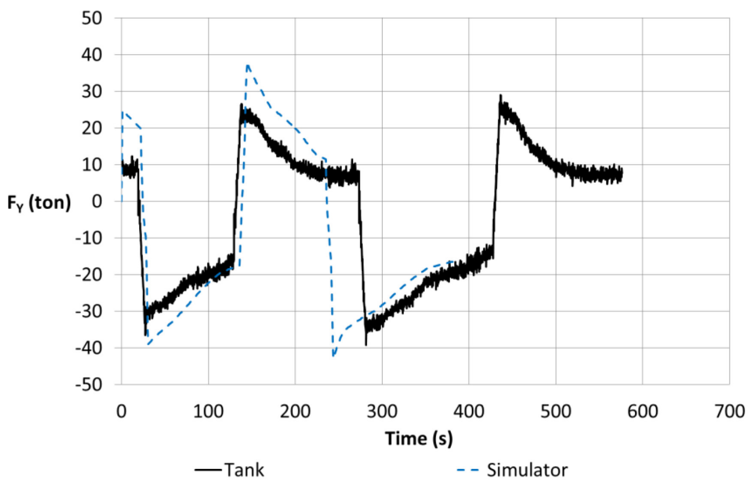


To test the rudder forces during captive manoeuvring tests a new test program has been executed, which will be discussed in a future report.

# 7 Conclusions and recommendations

This report described the implementation of a new C# autopilot in the Towing Tank for Manoeuvres in Confined Water after the refurbishment of the carriage's power. Free running tests have been carried out successfully using the benchmark container ship KCS. Regstatx has been adapted to post process free running tests, including the determination of PID constants for track following. The presently implemented controller is a variant of the controller that has been developed in the frame of a Master thesis in 2014. It is recommended to issue a follow up thesis to enhance this controller. At the same time the autopilot still needs testing with a twin rudder, twin propeller ship, including asymmetric tests with such configuration.

The repeatability of the free running tests has been checked. Some parameters of the zigzag test seem definitely affected by the initial roll angle, but not drastically. A more serious concern is the comparison with the simulations runs, where lower zigzag periods are obtained due to larger simulated rudder forces compared to those measured in the free running tests. It is imperative to research this matter with more detail, therefore in May 2018 additional captive tests are carried out with the KCS to investigate these rudder forces and possibly enhance their prediction. This will reported later in 2018.

# 8 References

**Delefortrie, G.; Eloot, K.; Mostaert, F.** (2018). Manoeuvring models: sub report 5. Manoeuvring model for a Q-flex LNG carrier. Version 3.. *FHR reports*, 16_023_5. Flanders Hydraulics Research: Antwerp

**Reynvoet, T.** (2014). Design of an autopilot for free running ship models. Department of Civil Engineering, Ghent University. 1-209 pp.

**Fossen, T. I.** (2018). Guidance and Control of Vehicles. Chapter 12, Motion Control Systems. http://www.fossen.biz/wiley/Ch12.pdf (Last accessed: April 20, 2018).

# Appendix 1: free running zigzag tests

## Time traces

Figure 18 - Free running time traces of -10/2.5 zigzag tests at 50% ukc

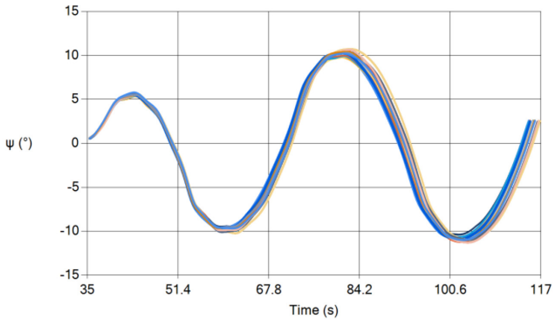


a. Course angle

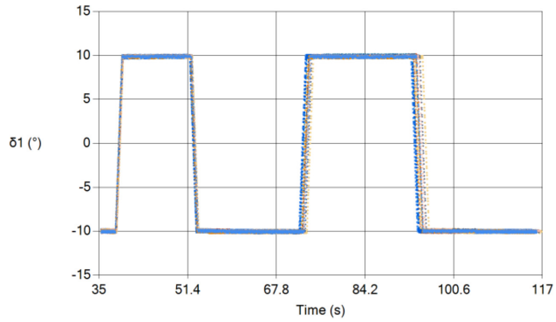


b. Rudder angle

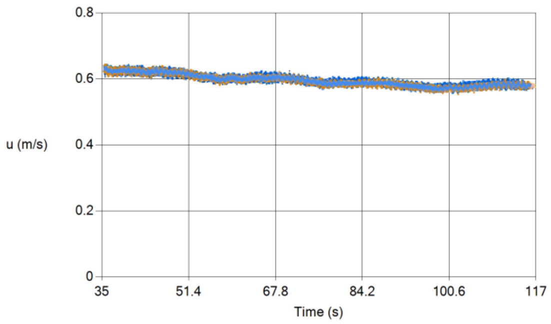


c. Longitudinal speed

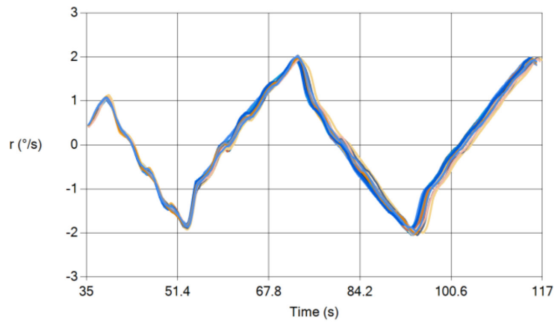


d. Yaw rate

Figure 19 - Free running time traces of 10/2.5 zigzag tests at 50% ukc

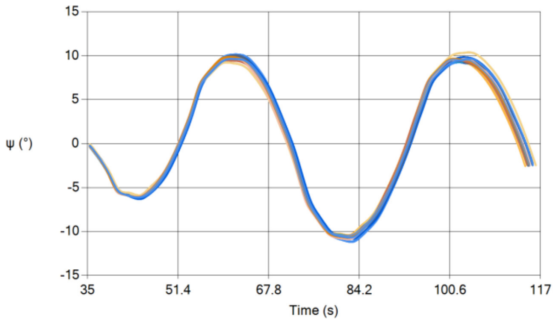


a. Course angle

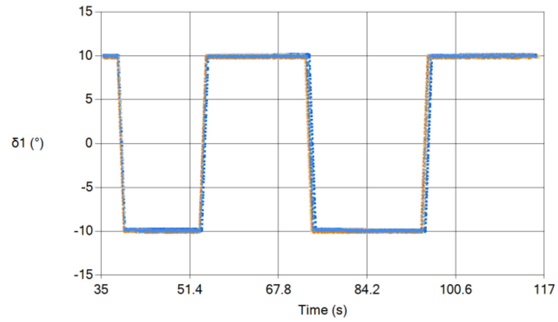


b. Rudder angle

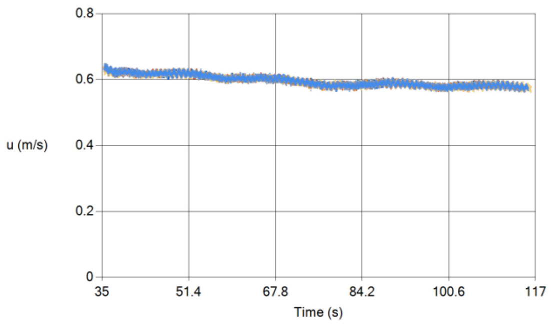


c. Longitudinal speed

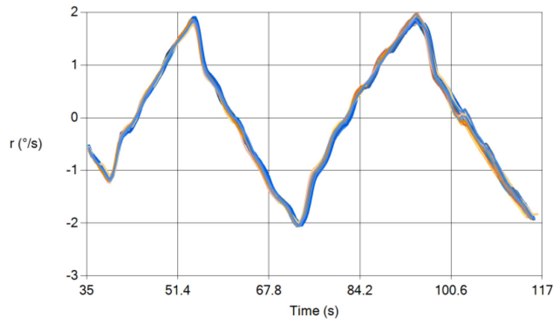


d. Yaw rate

Figure 20 - Free running time traces of -20/5 zigzag tests at 50% ukc

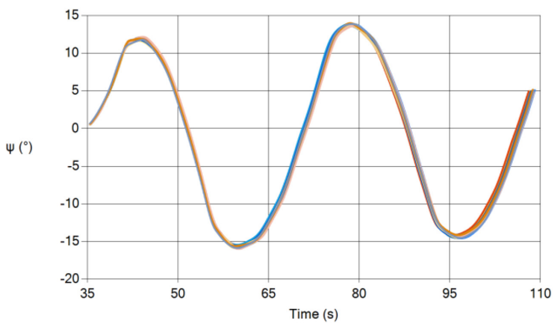


a. Course angle

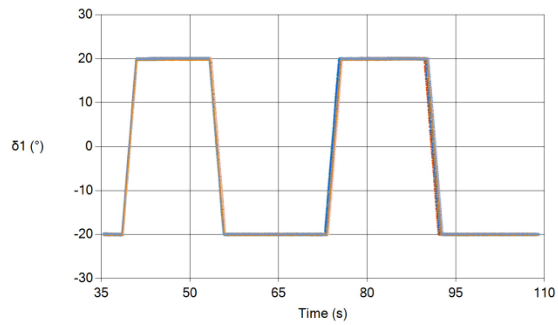


b. Rudder angle

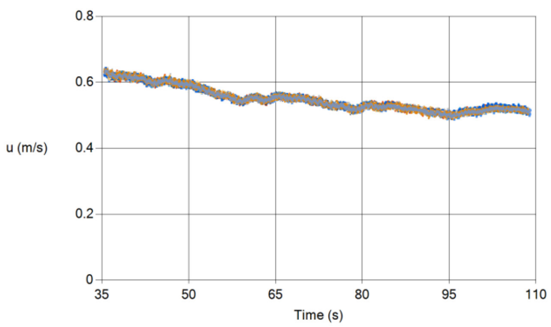


c. Longitudinal speed

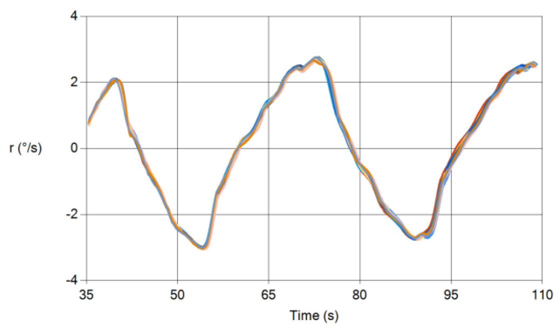


d. Yaw rate

Figure 21 - Free running time traces of 20/5 zigzag tests at 50% ukc

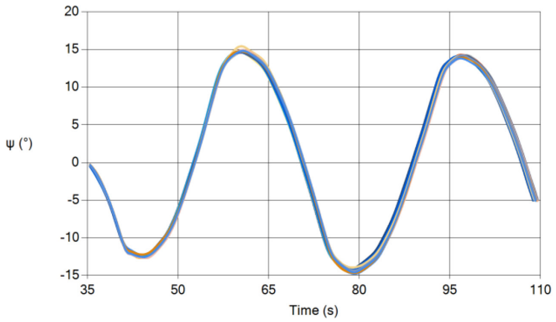


a. Course angle

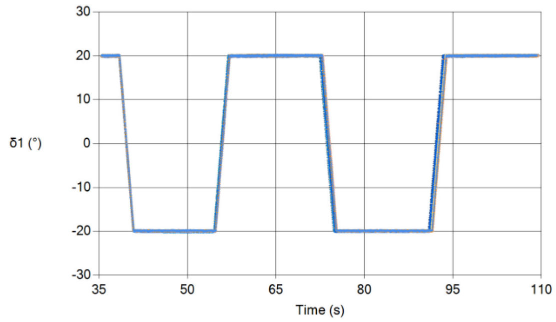


b. Rudder angle

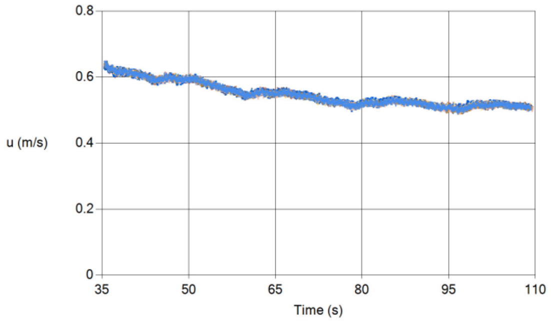


c. Longitudinal speed

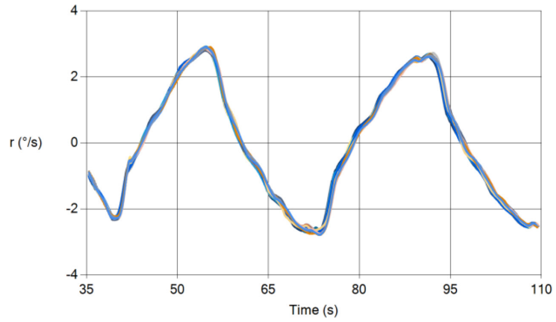


d. Yaw rate

Figure 22 - Free running time traces of -10/2.5 zigzag tests at 20% ukc

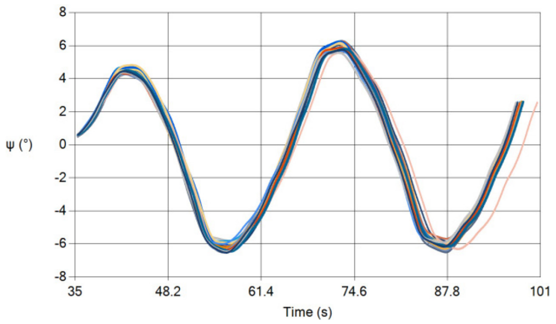


a. Course angle

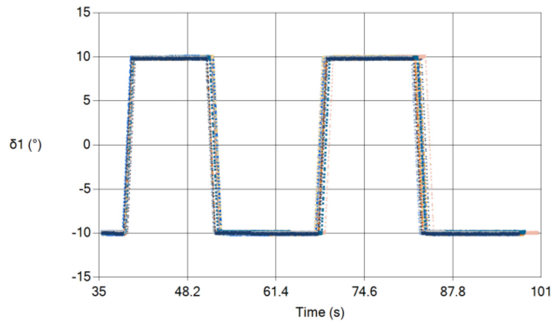


b. Rudder angle

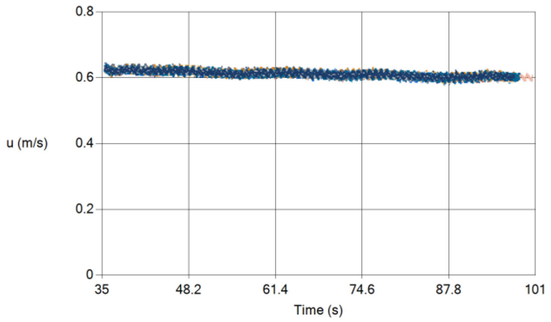


c. Longitudinal speed

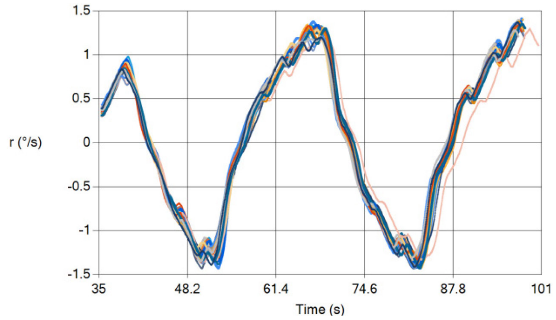


d. Yaw rate

Figure 23 - Free running time traces of 10/2.5 zigzag tests at 20% ukc

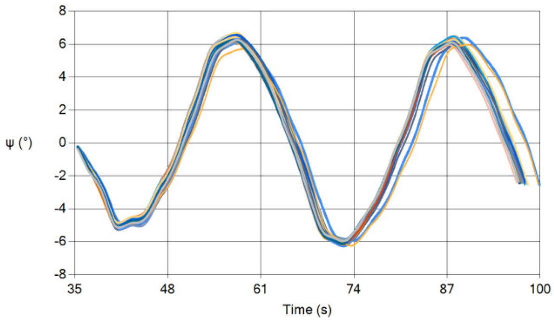


a. Course angle

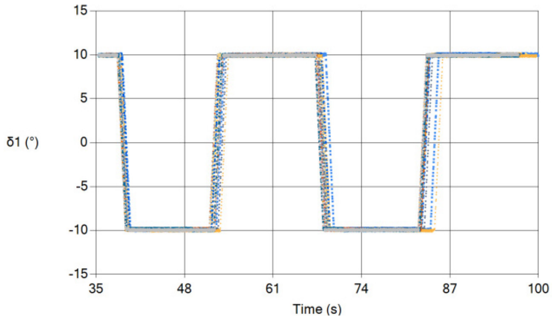


b. Rudder angle

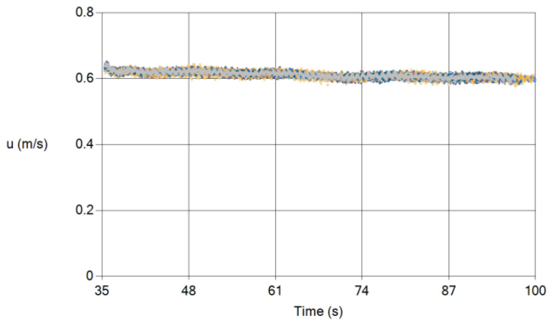


c. Longitudinal speed

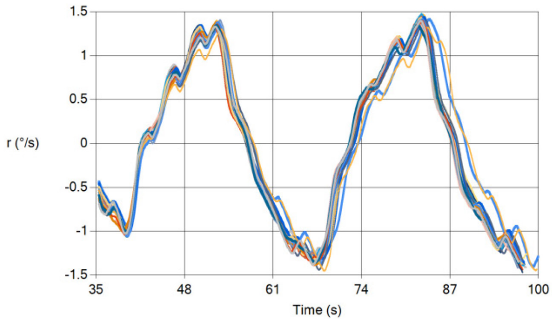


d. Yaw rate

Figure 24 - Free running time traces of -20/5 zigzag tests at 20% ukc

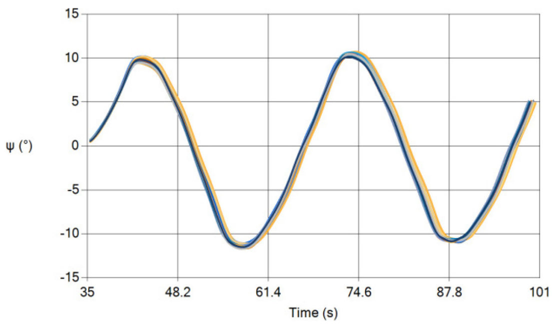


a. Course angle

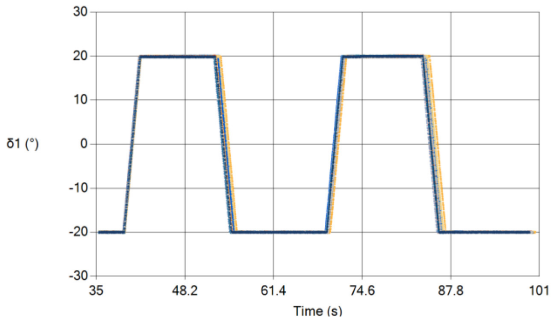


b. Rudder angle

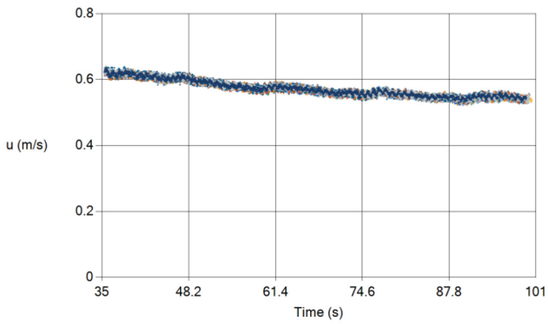


c. Longitudinal speed

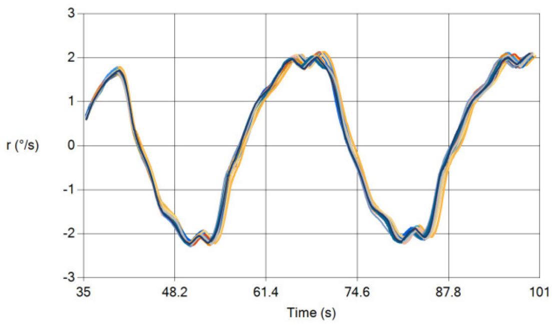


d. Yaw rate

Figure 25 - Free running time traces of 20/5 zigzag tests at 20% ukc

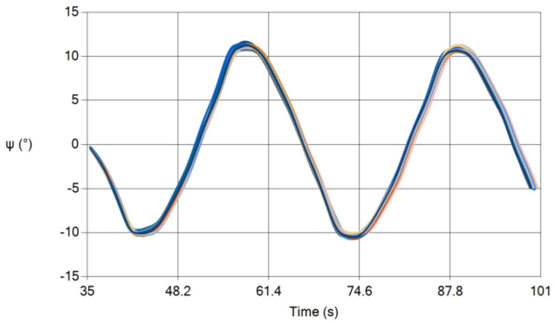


a. Course angle

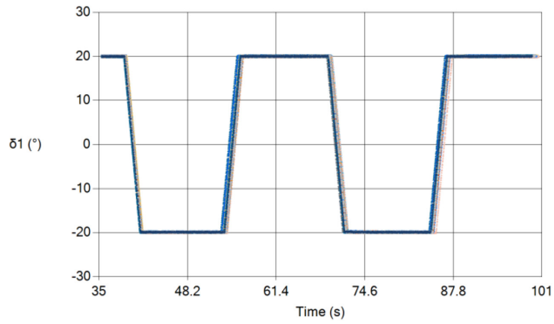


b. Rudder angle

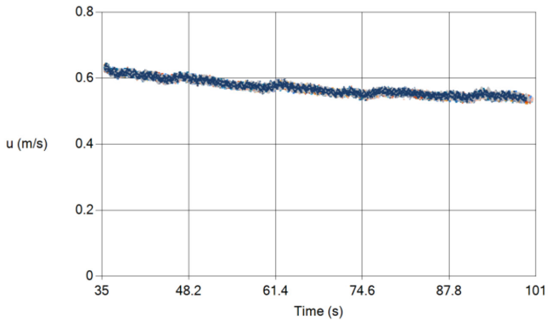


c. Longitudinal speed

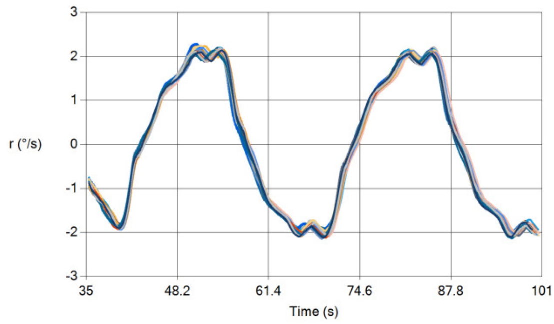


d. Yaw rate

# Statistics

Figure 26 - Statistics of 10/2.5 zigzag tests at 50% ukc

Starting to portside | Starting to starboard side

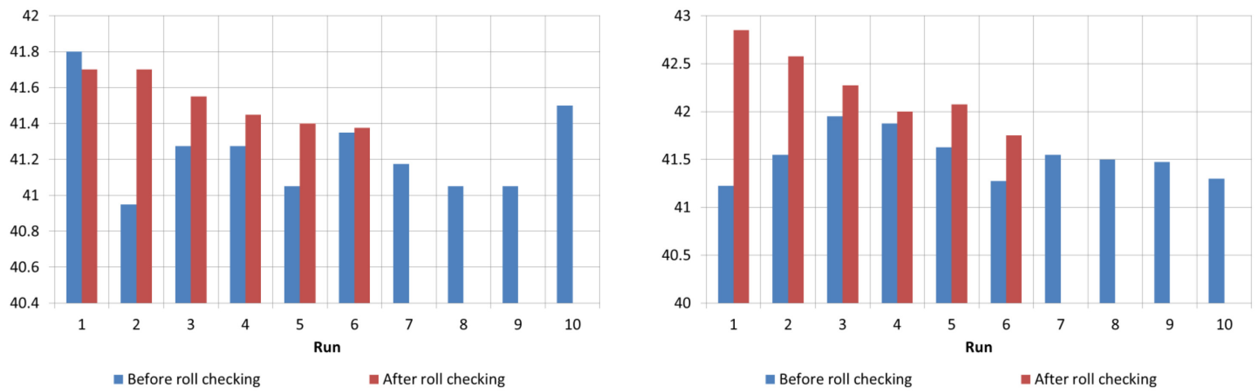


a. Period

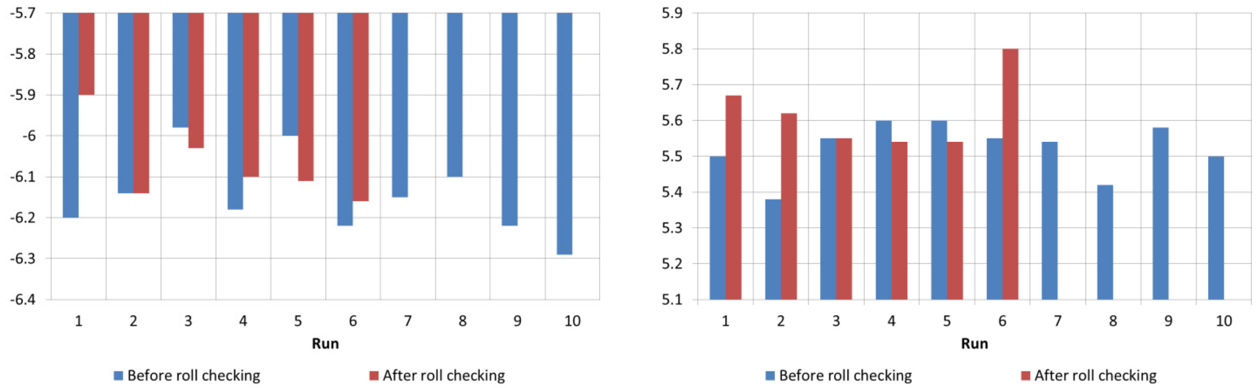


b. First maximal course angle

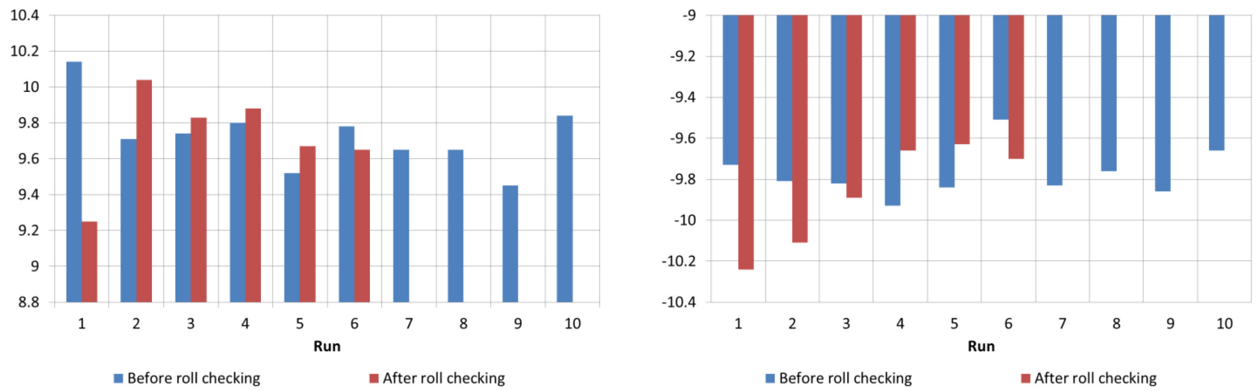


c. Second maximal course angle

Figure 27 - Statistics of 20/5 zigzag tests at 50% ukc

Starting to portside | Starting to starboard side

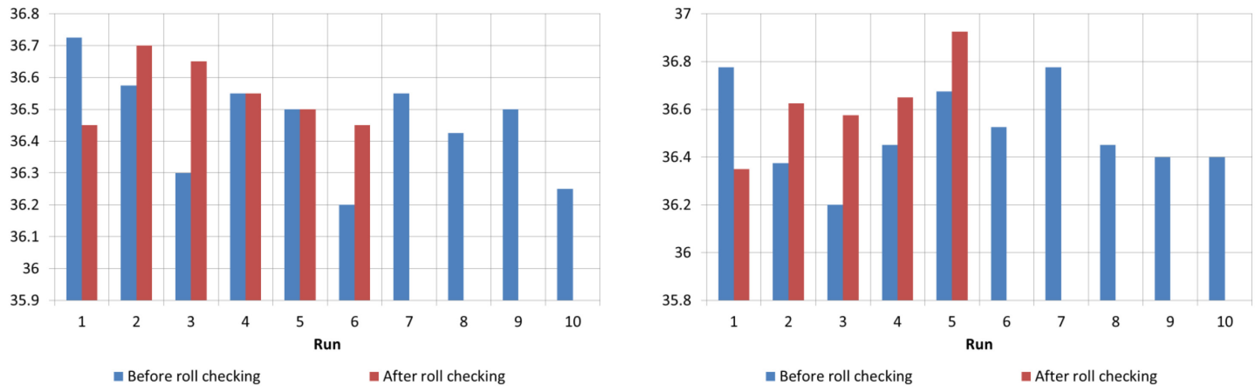


a. Period

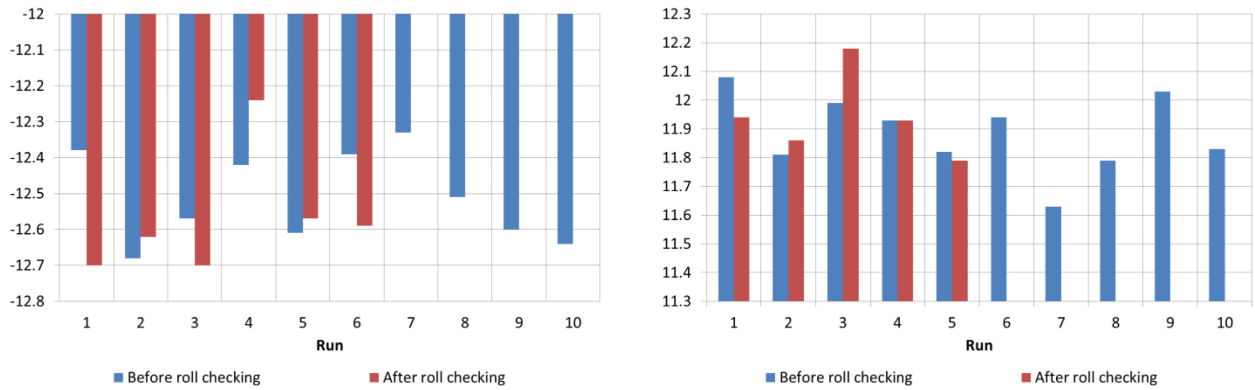


b. First maximal course angle

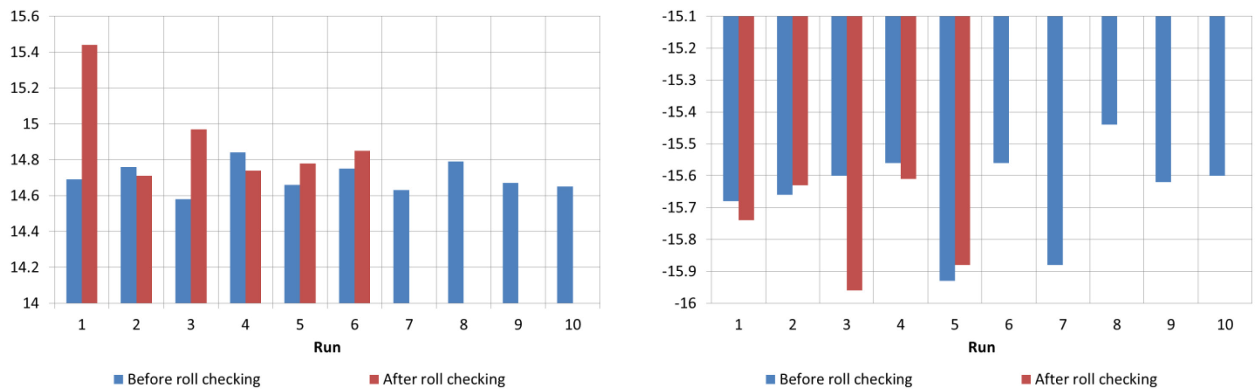


c. Second maximal course angle

Figure 28 - Statistics of 10/2.5 zigzag tests at 20% ukc

Starting to portside | Starting to starboard side

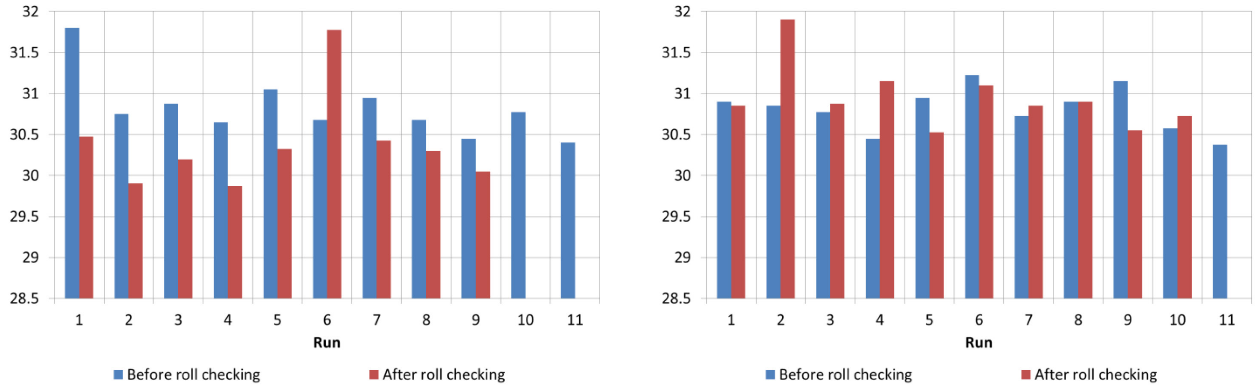


d. Period

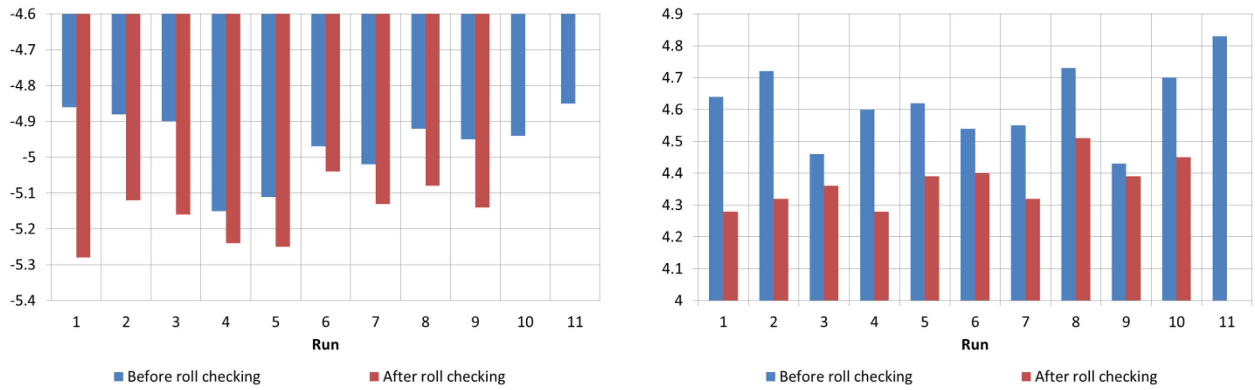


e. First maximal course angle

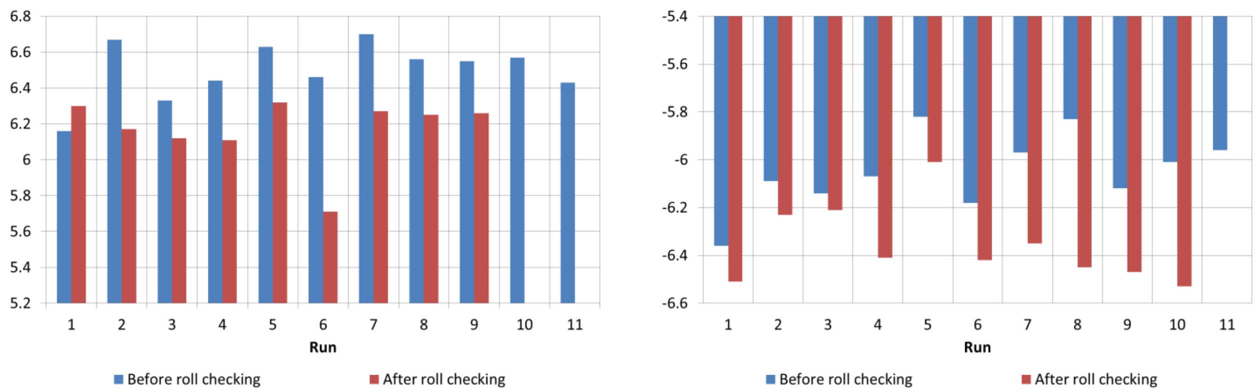


f. Second maximal course angle

Figure 29 - Statistics of 20/5 zigzag tests at 20% ukc

Starting to portside | Starting to starboard side

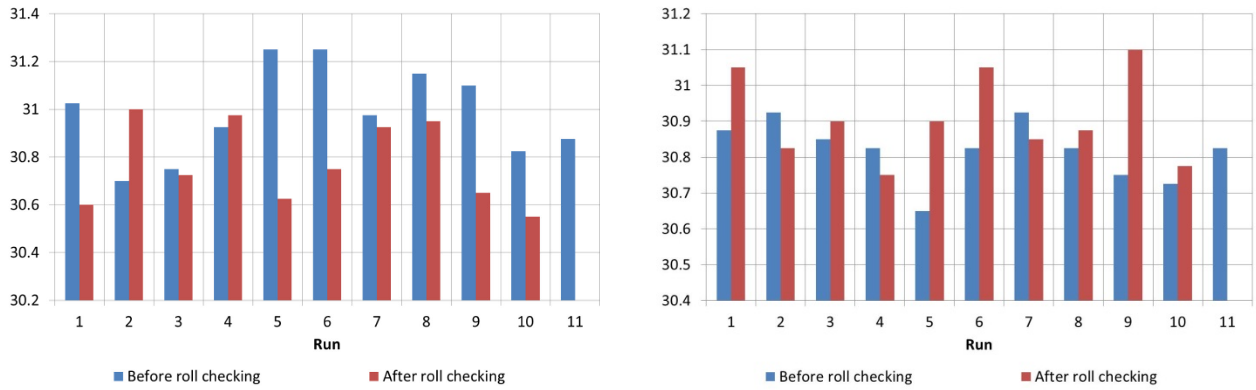


a. Period

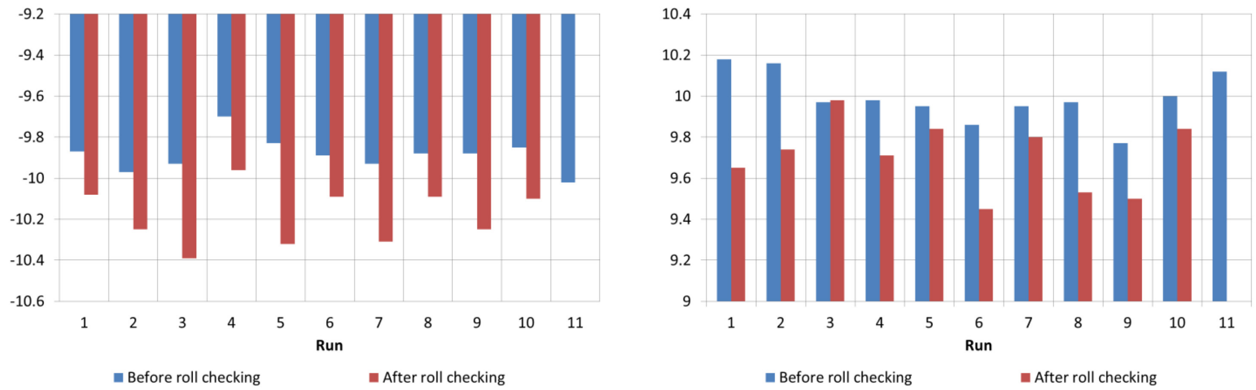


b. First maximal course angle

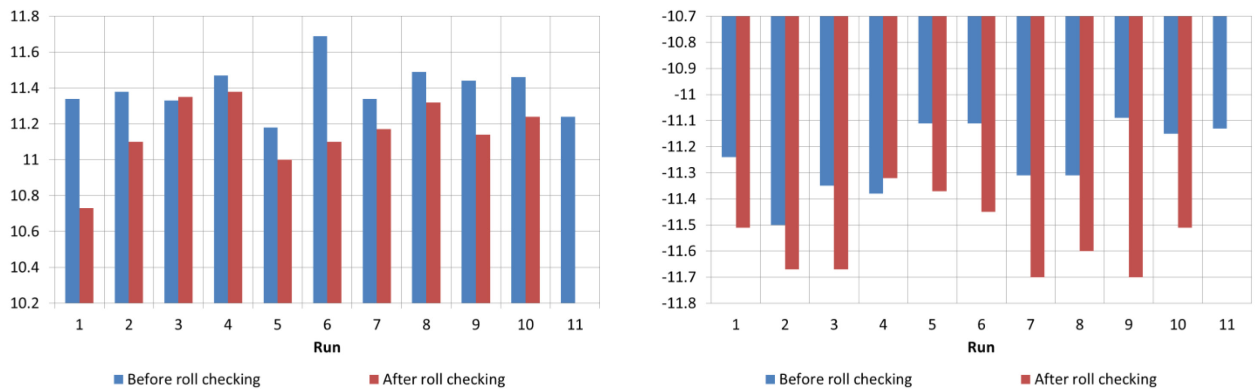


c. Second maximal course angle

# Appendix 2: comparison between free running and simulated zigzag tests

Figure 30 – Comparison between free running and simulated -10/2.5 zigzag test at 50% ukc

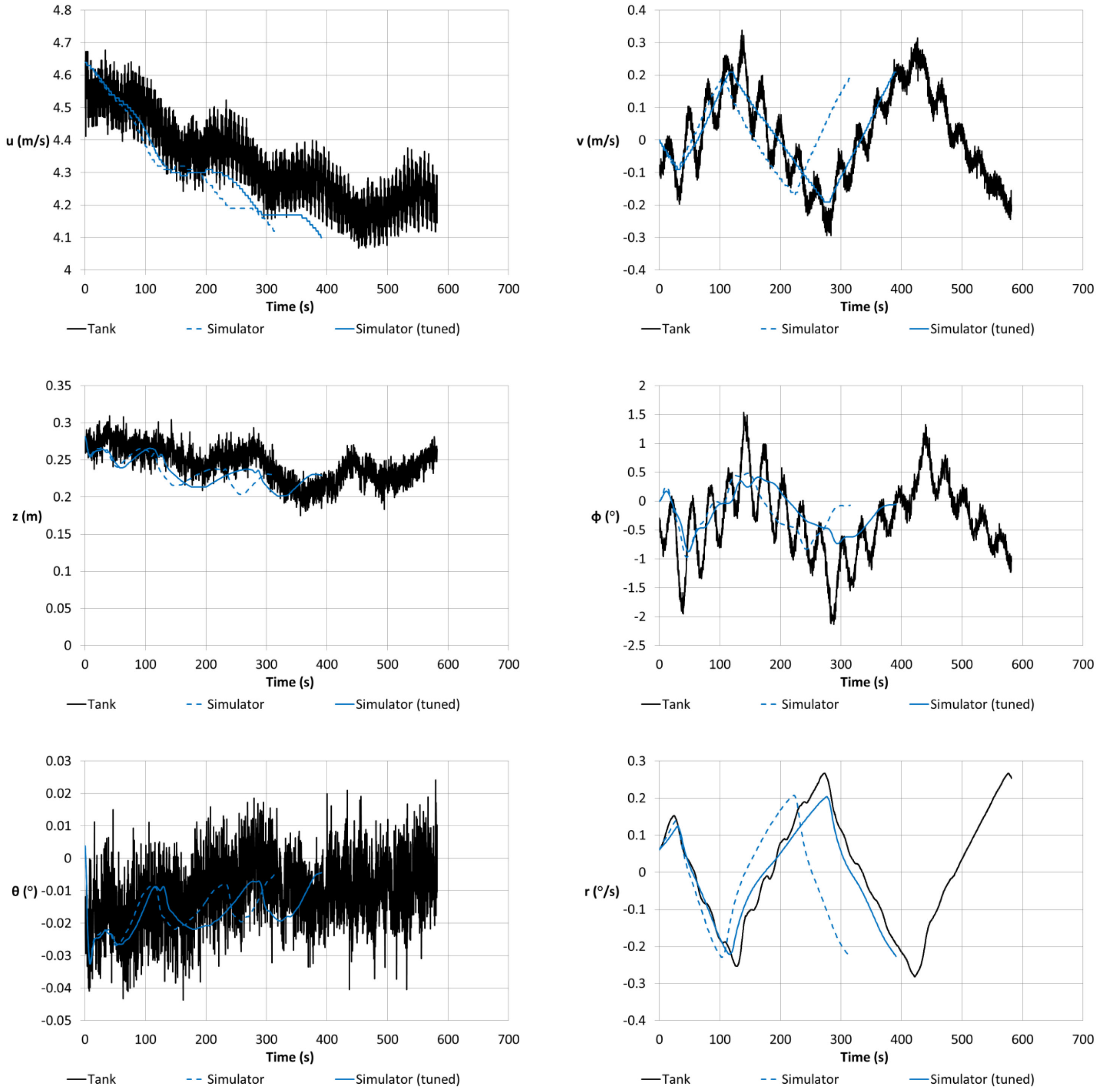

Figure 31 – Comparison between free running and simulated 10/2.5 zigzag test at 50% ukc

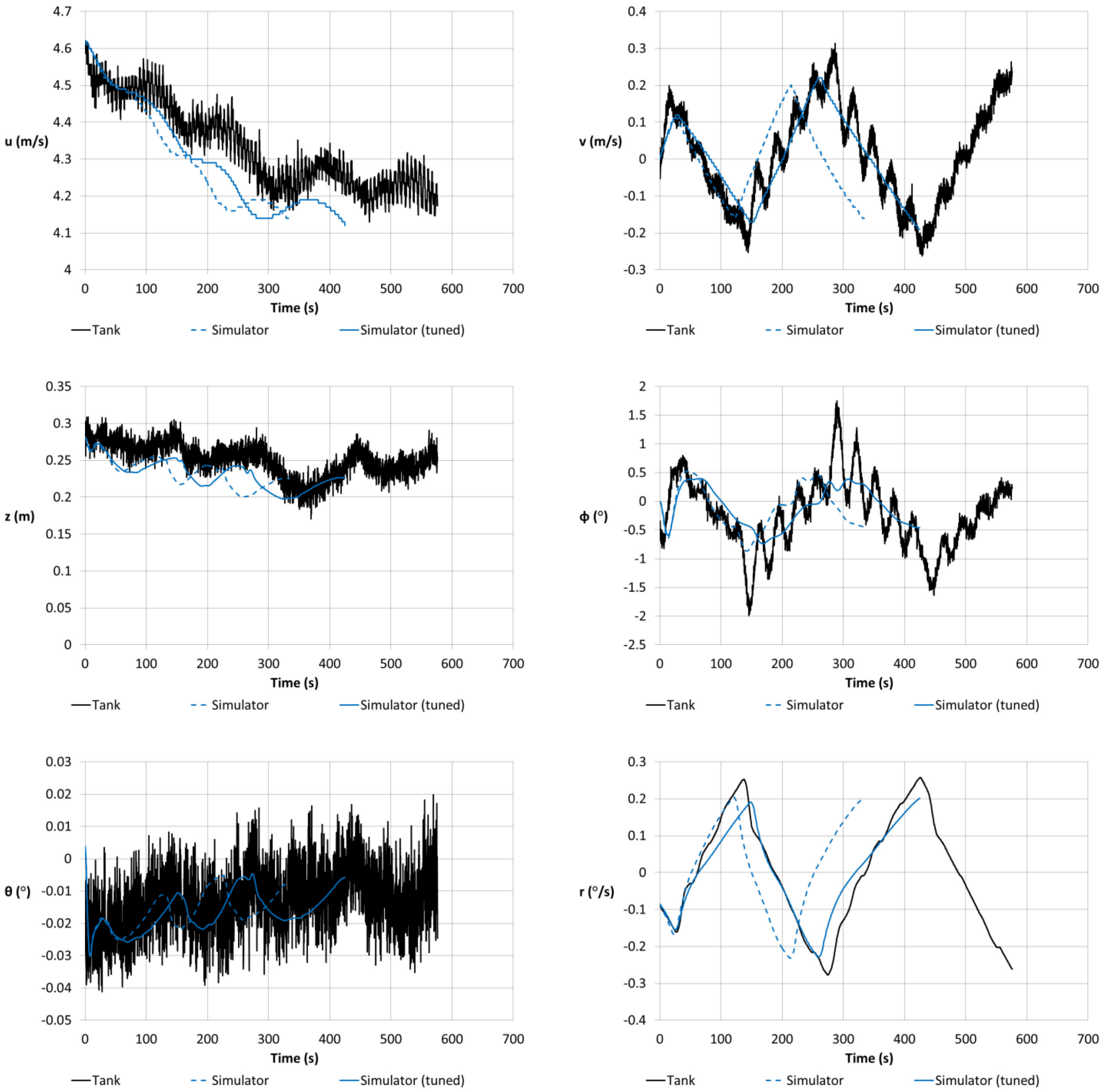

Figure 32 – Comparison between free running and simulated -20/5 zigzag test at 50% ukc

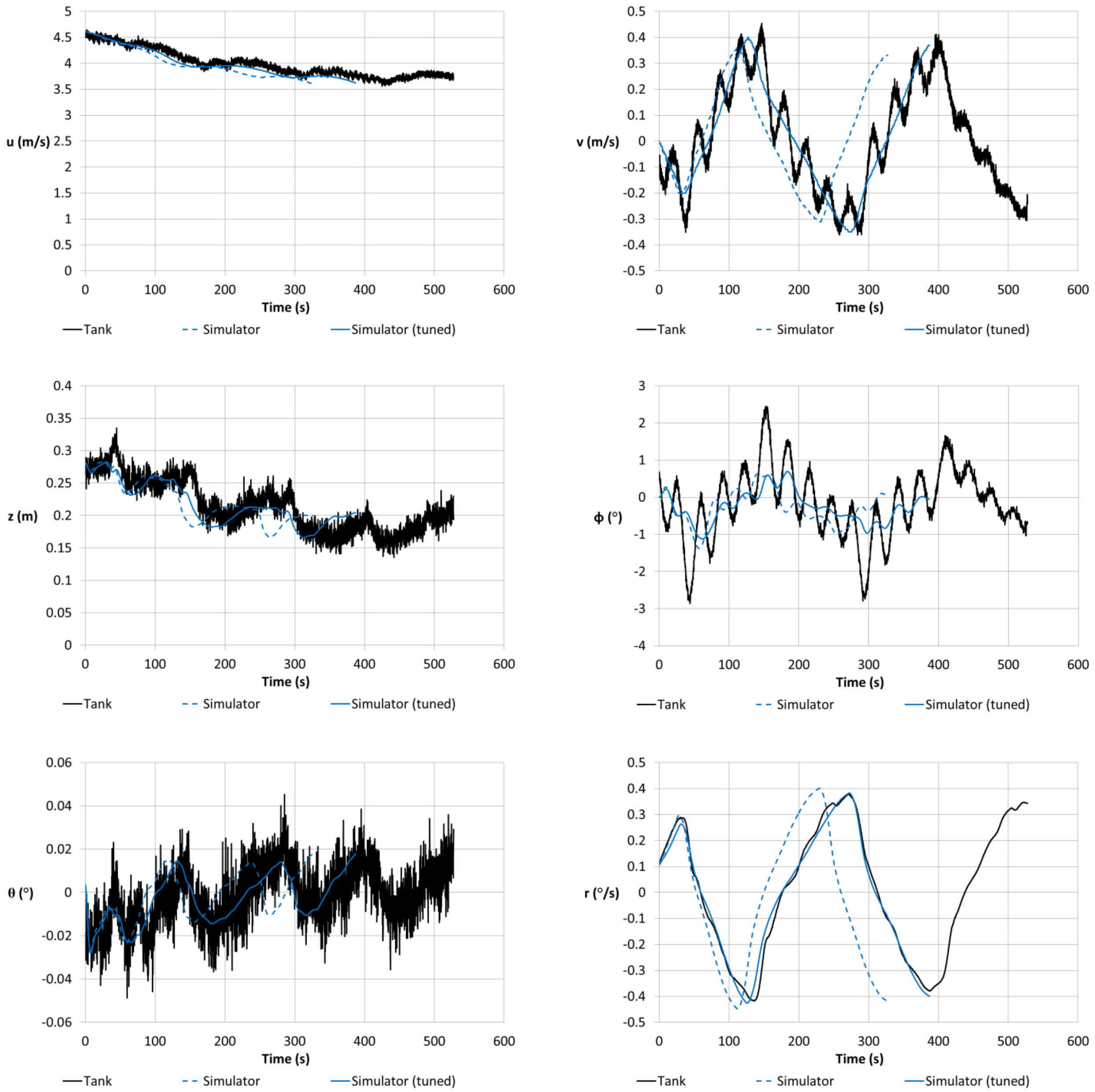

Figure 33 – Comparison between free running and simulated 20/5 zigzag test at 50% ukc

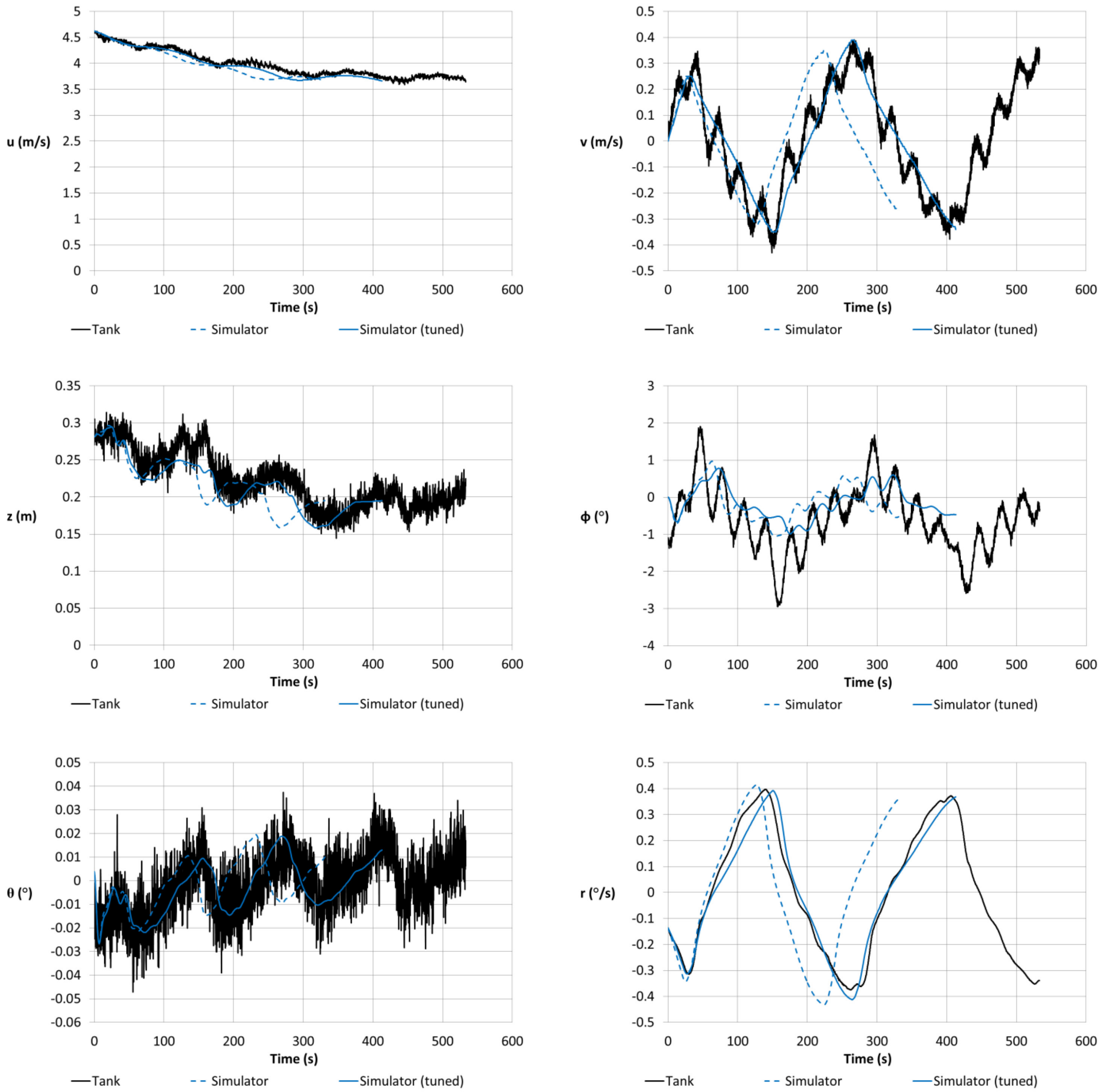

Figure 34 – Comparison between free running and simulated -10/2.5 zigzag test at 20% ukc

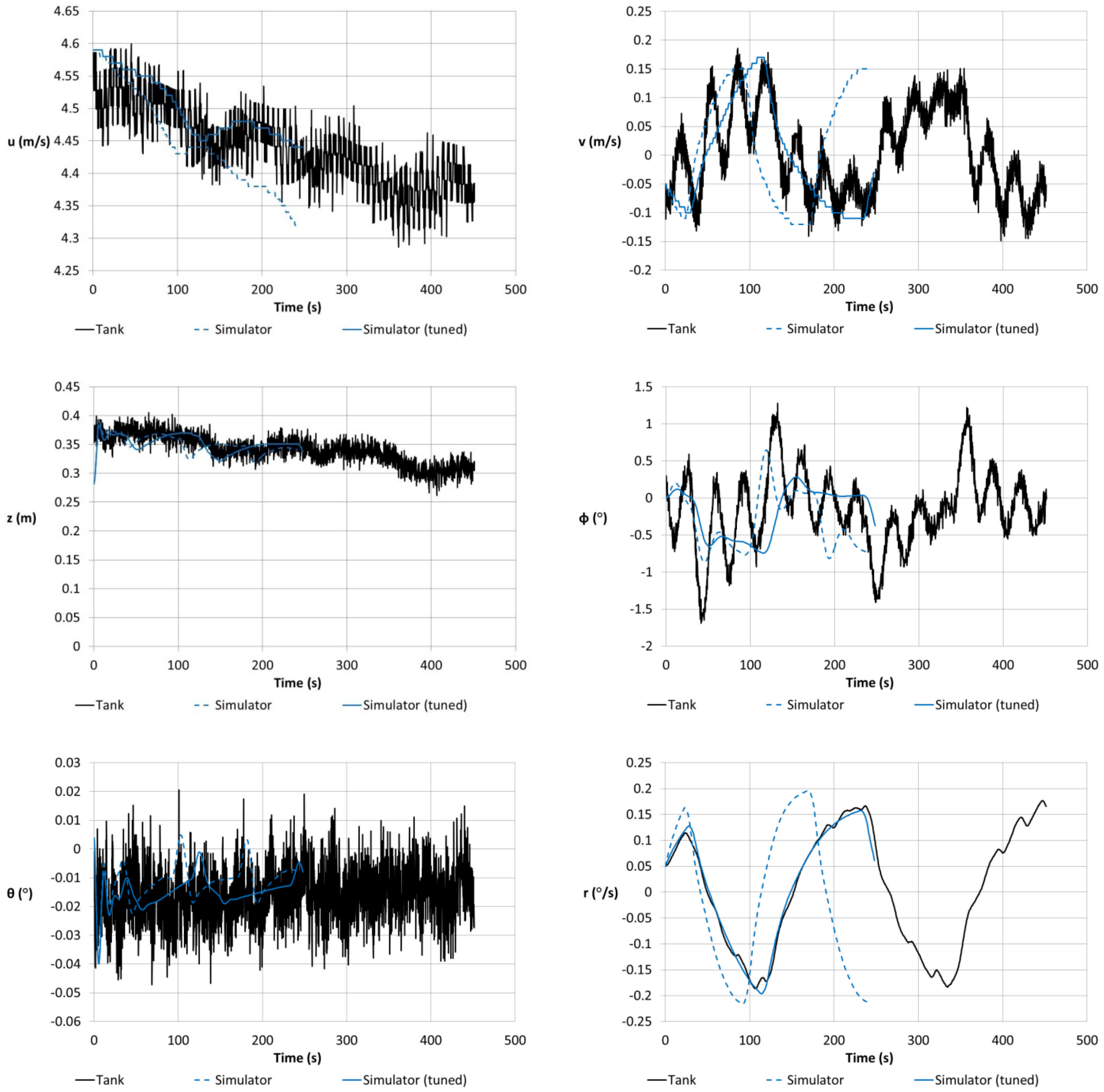

Figure 35 – Comparison between free running and simulated 10/2.5 zigzag test at 20% ukc

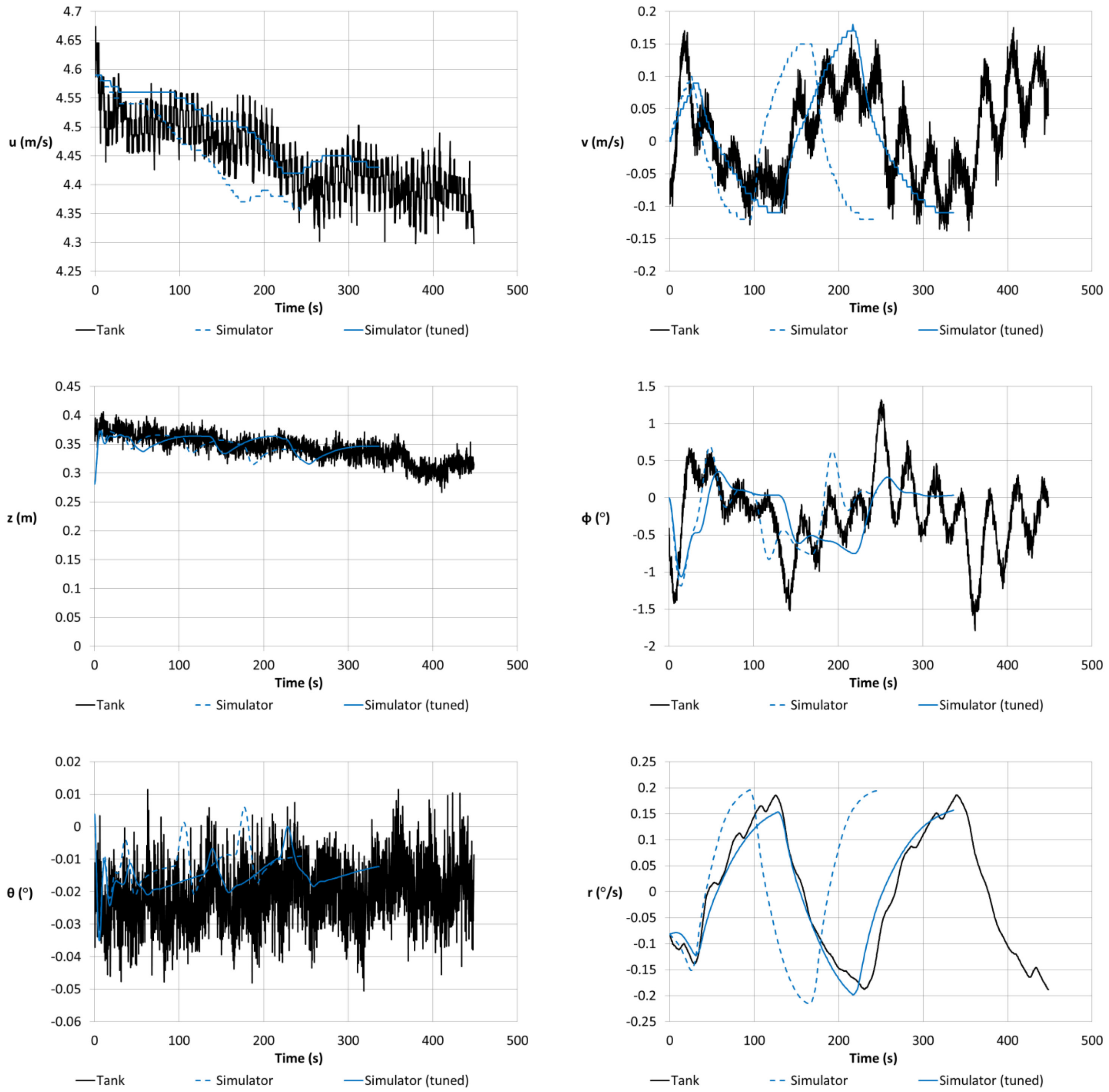

Figure 36 – Comparison between free running and simulated -20/5 zigzag test at 20% ukc

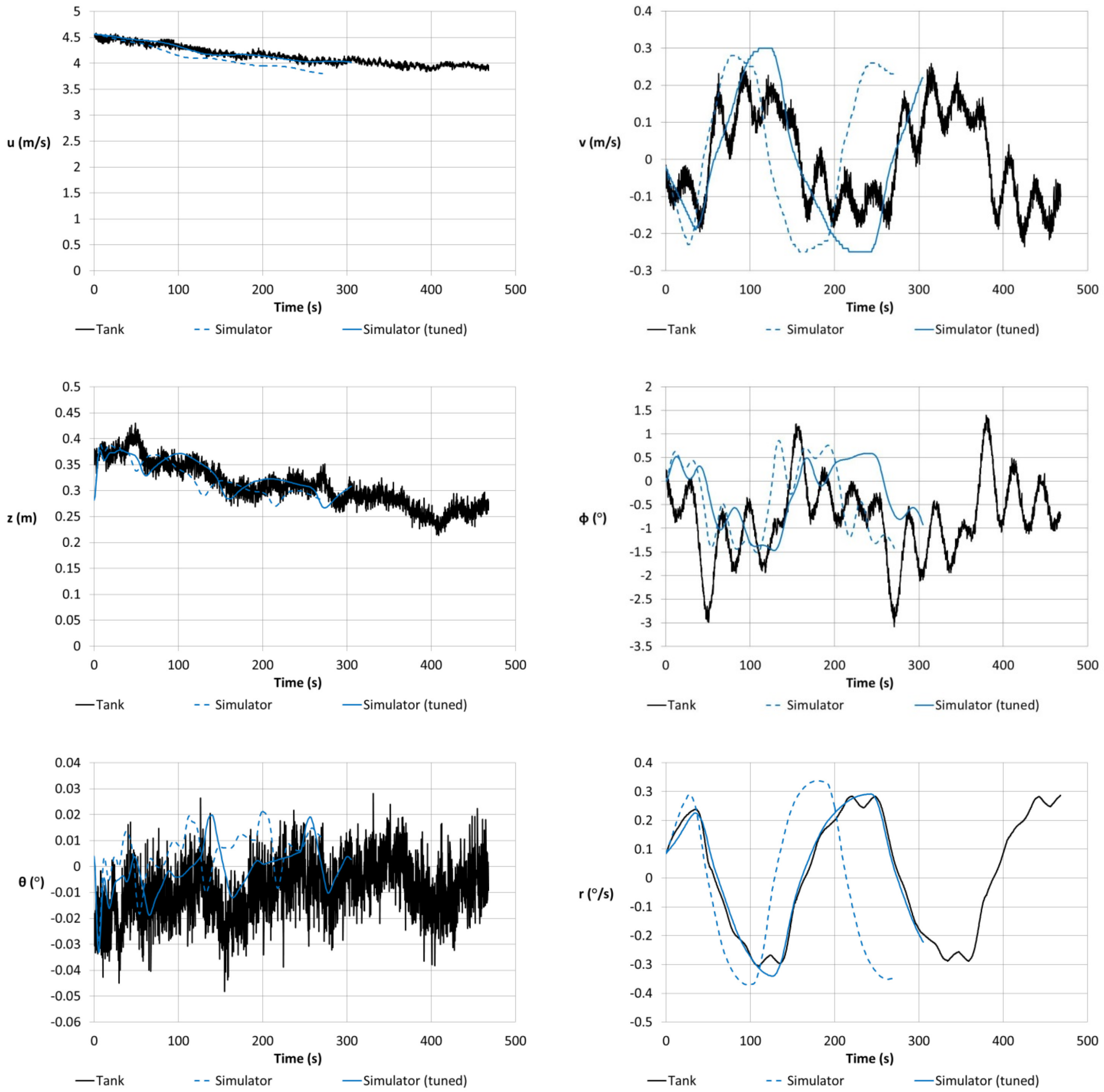

Figure 37 – Comparison between free running and simulated 20/5 zigzag test at 20% ukc

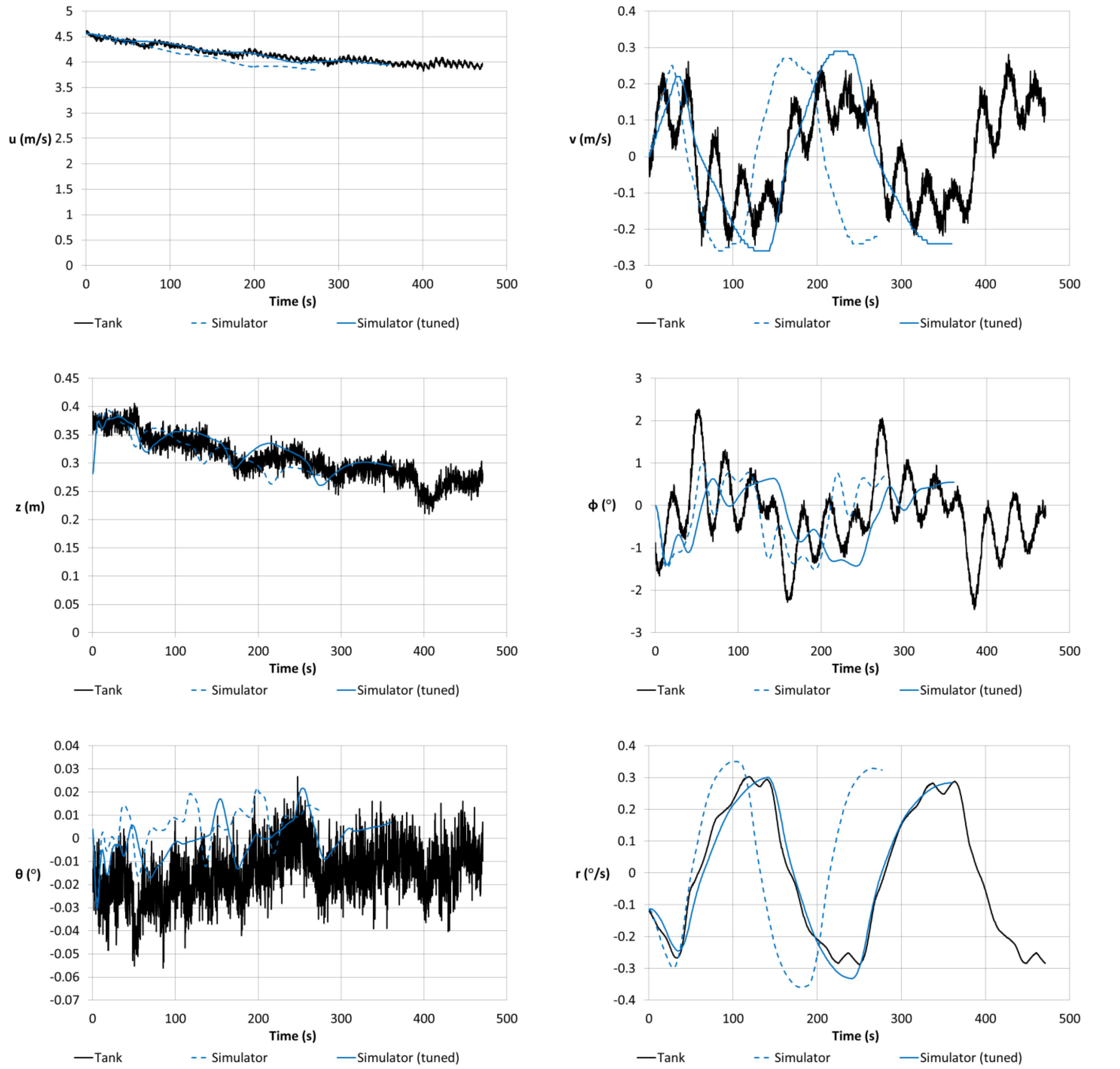

DEPARTMENT **MOBILITY & PUBLIC WORKS**
Flanders hydraulics Research

Berchemlei 115, 2140 Antwerp
**T** +32 (0)3 224 60 35
**F** +32 (0)3 224 60 36
waterbouwkundiglabo@vlaanderen.be
**www.flandershydraulicsresearch.be**